A STUDY OF WIRE MESH WICK CHARACTERISTICS IN A LONGITUDINAL HEAT PIPE

Oscar Jonathan Hickox

United States
Naval Postgraduate School

THESIS

A STUDY OF WIRE MESH WICK CHARACTERISTICS

IN A LONGITUDINAL HEAT PIPE

by

Oscar Jonathan Hickox, Jr.

December 1969

A Study of Wire Mesh Wick Characteristics In a Longitudinal Heat Pipe

by

Oscar Jonathan Hickox, Jr.
Lieutenant, United States Navy
B.S., United States Naval Academy, 1962

Submitted in partial fulfillment of the
requirements for the degree of

MASTER OF SCIENCE IN MECHANICAL ENGINEERING

from the

NAVAL POSTGRADUATE SCHOOL
December 1969

ABSTRACT

An everted, glass-enclosed, nickel heat pipe was operated at constant volume using a nickel wire mesh wick and distilled water. The performance of the pipe was evaluated under various combinations of wick parameters. The effect of the radial evaporator capillary radius, the radial condenser capillary radius, and the evaporator wetting angle were investigated at a pressure range of 27 to 24 inches of Mercury vacuum.

The performance of the pipe was found to improve with decreasing radial evaporator capillary radius and decreasing amounts of non-condensables in the working fluid. A detrimental wick-aging effect which led to violent boiling and early dryout was observed.

A discussion of observed behavior presents evidence that boiling and wick fin effect may play a significant part in heat pipe operation.

TABLE OF CONTENTS

LIST OF TABLES

LIST OF FIGURES

TABLE OF SYMBOLS

A	Cross-sectional area, in^2
C	Arbitrary constant, various
H	Latent heat of vaporization, BTU/lbm
K_1	Friction factor, in^{-2}
L	Length, in, ft
P	Pressure, lbf/in^2
Q	Heat transfer rate, BTU/sec, watts
V	Average velocity, ft/sec
d	Diameter, in
ht	Height, in
k	Thermal conductivity, BTU/ft-hr-°F
r	Radius, in
Δ	Difference
θ	Wetting angle, degrees
μ	Viscosity, $lbf\text{-}sec/ft^2$
ρ	Density, lbm/ft^3
σ	Surface tension, lbf/in
$\propto$	Proportional to

Subscripts

c	capillary
e	evaporator
f	frictional
g	glass wall
h	heater
i	inner

Subscripts Continued

l	liquid
m	meniscus
o	outer
p	pipe
s	spacing
t	total
u	upper
v	vapor
w	wick
cd	condenser
cs	cross-section
lm	logarithmic mean
lr	lower
mn	mean
pp	pumping
wr	wire
max	maximum
min	minimum

ACKNOWLEDGEMENTS

The author is indebted to Dr. P. F. Pucci of the Naval Postgraduate School for his encouragement and helpful guidance as thesis advisor. To Dr. P. J. Marto of the Naval Postgraduate School, sincere appreciation is offered for his continual interest, stimulating suggestions, and forthright encouragement without which this investigation would have proven much less fruitful. Appreciation is also due to the various technicians at the Naval Postgraduate School whose patient understanding and professional talents were significant contributions to the successful outcome of this endeavor. Notable among the above category was the glass blower, Mr. Robert C. Schiele, whose long hours and immediate responses to calls for assistance were indispensable.

I. INTRODUCTION

A. BACKGROUND

The heat pipe is a compact, simple apparatus which can transfer up to five hundred times as much thermal energy per unit weight as can a solid thermal conductor of the same cross-section [1]. The principles of operation of the heat pipe can be described by the well-established laws of thermodynamics, heat transfer, and fluid mechanics. However, many interesting areas of heat pipe operation have yet to be fully explained.

The first published article on heat pipes was authored by G. M. Grover et al in 1964 [2]. Since that time, most research efforts have been directed toward high-capacity, high-temperature pipes using liquid metals as operating fluids. Less effort has been expended in investigating less sophisticated, low-temperature pipes using common, economical fluids such as water and alcohol.

A simple, cheap heat pipe can be easily constructed by rolling a porous media (such as wire mesh) into an annular shape, placing it inside a pipe, adding some water, and capping the ends. Such pipes have been constructed and are easily designed for low-capacity applications [1].

The economic advantages of employing low-cost pipes are obvious. However, as is typically the case with cheaply constructed equipment, these pipes tend to produce relatively low performance. The wire mesh wick, while easy to assemble, has a characteristic disadvantage, notably high resistance to fluid flow. It has been shown by W. L. Mosteller that the operation of a low-performance pipe using a wire mesh wick is limited by the pumping performance of the wick [3]. The performance of

the wick therefore becomes of primary interest in any effort to maximize heat pipe efficiency.

Some earlier investigations have centered upon wick performance. Mosteller [3], and Kilmartin [4] have shown that heat pipe performance is improved by operating at higher pressures, by proper choice of working fluid, and by optimizing wick thickness and characteristic capillary radius. It has been known for some time that the wick capillary radius and the wick-liquid wetting angle are major factors in the performance of a heat pipe [1]. To date no effort has been made to subdivide the capillary radius and the wetting angle into independent parameters, according to location in the wick and directional influence, in order to optimize wick performance. A study of wick characteristics defined in terms of these subdivided parameters could lead to methods for adapting these characteristics to more efficient heat pipe operation.

B. THESIS OBJECTIVES

The objectives of this study were to determine theoretically the characteristics affecting wire mesh wick operation, to show how these characteristics could be varied to improve wick operation, and to conduct practical experiments on a heat pipe to verify, qualitatively, that the performance of a heat pipe is improved by properly varying these characteristics.

II. HEAT PIPE THEORY

A. TERMINOLOGY

In order to discuss the operation of a heat pipe, certain descriptive terms must be defined. The following is a list of terms basic to the understanding of heat pipe operation:

Capillary Pump - The action in which the wick affects the transfer of fluid from the condenser to the evaporator.

Capillary Radius - The porous character of the wick is described in terms of an effective or equivalent radius of a capillary tube.

Condenser - Section of the pipe where heat is removed.

Dryout - Synonomous with Break-Point and Burnout-Point. Dryout occurs when the wick cannot return fluid to the evaporator at the rate at which it is evaporated. This condition is indicated by a continual temperature rise in the evaporator. It is not necessarily accompanied by a physically dry wick.

Evaporator - Section of the pipe where heat is added.

Friction Factor - A factor of dimensions $(\text{length})^{-2}$ related to the internal wick resistance to fluid flow.

Wetting Angle - Angle of contact between the wick surface and the line-of-action of the liquid surface tension at the point of contact.

Wick - Porous media which contains the working fluid.

Working Fluid - Fluid contained in the wick and vapor space, is the means by which energy is transported.

B. GENERAL - The Horizontal, Everted Heat Pipe with Wire Mesh Wick.

The basic mechanisms by which the heat pipe transfers heat can be described schematically as in Figure 1.

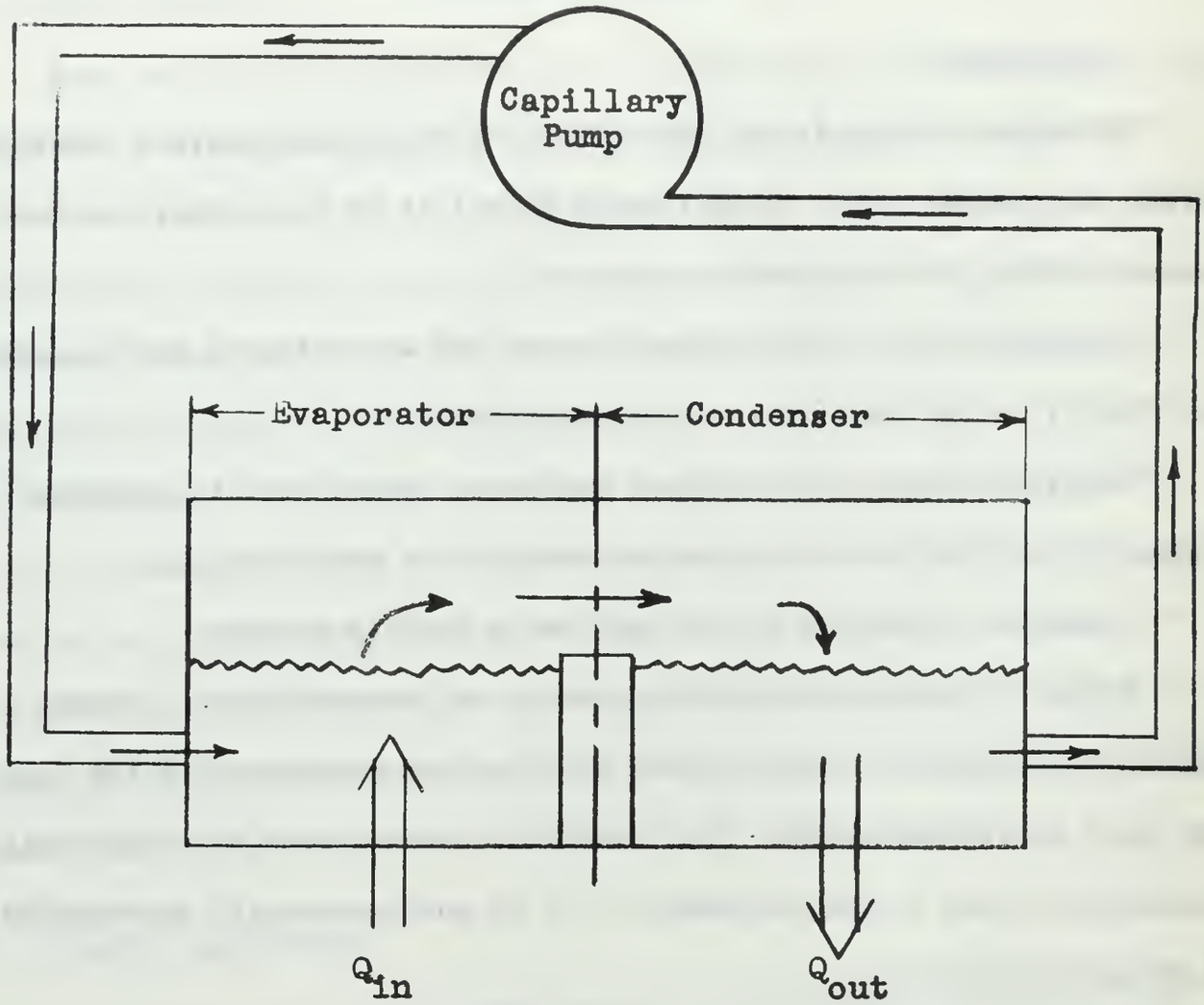

Figure 1. Schematic of a Basic Heat Pipe Flow Cycle

There are four basic functions which must be considered in developing heat pipe theory:

1. Liquid pumping performed by the capillary pump.
2. Fluid flow resistance of the flow path.
3. Radial heat conduction in the condenser and evaporator.
4. Liquid-vapor flow separation at high performance conditions.

This study does not involve operation at high performance conditions, so factor number four will not be considered in developing the theory of

operation. Factor number three is a function of the radial thermal conductivity properties of the wick-liquid combination and will be considered in part D of Heat Pipe Theory, Radial Heat Transfer. Factors number one and two are explored in detail in part C, Wick Operation. The basic theory of operation is developed in the following analysis.

Around any closed path on the inside of the heat pipe, the sum of the pressure changes must equal zero.

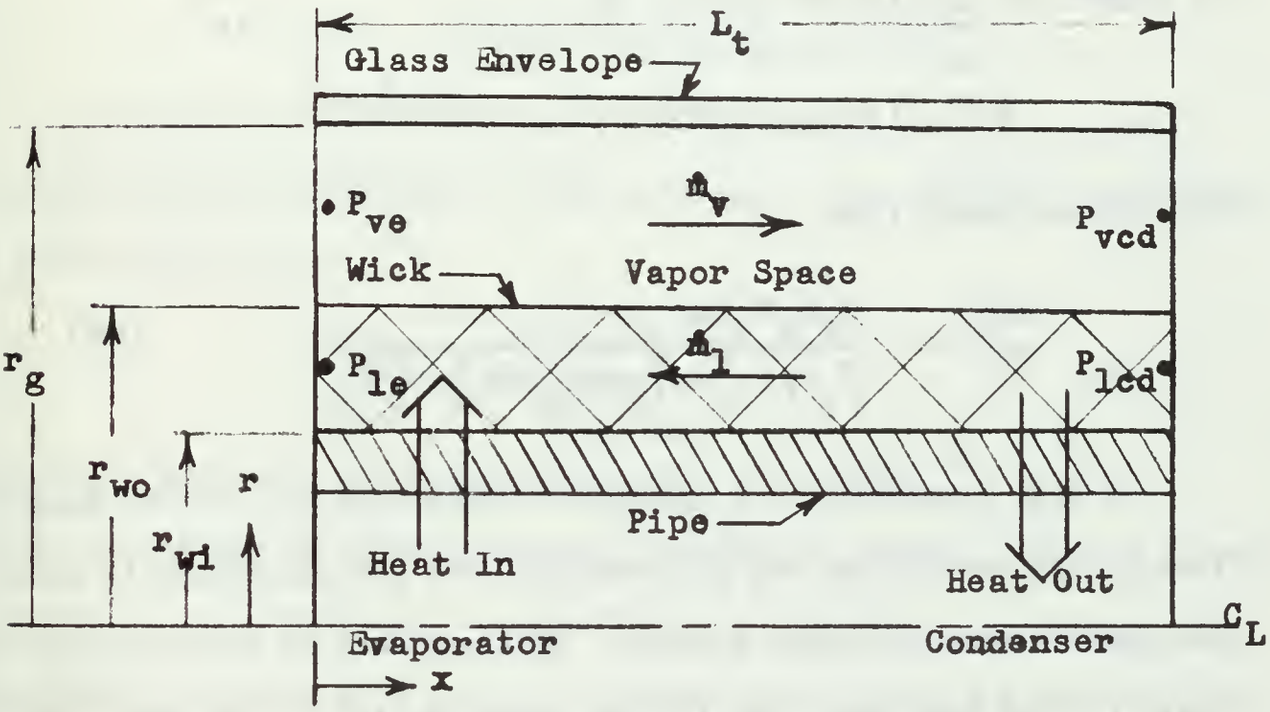

Figure 2. Schematic of an Everted Heat Pipe Flow Cycle

Referring to Figure 2,

$$(P_{ve}-P_{vcd})+(P_{vcd}-P_{lcd})+(P_{lcd}-P_{le})+(P_{le}-P_{ve})=0 \qquad (1)$$

The first term in equation (1) represents the change in vapor pressure from the evaporator to the condenser. For fully developed, steady, laminar, incompressible flow in an annulus with axial direction x [5],

$$\frac{dP}{dx} = - \frac{8\mu V}{r_o^2+r_i^2-2r_{lm}^2} \qquad (2)$$

where $$r_{lm} = \left[\frac{r_o^2-r_i^2}{\ln(r_o/r_i)^2} \right]^{\frac{1}{2}}$$

By continuity for steady flow,

$$\dot{m} = V \rho A_{cs} \text{ , where } A_{cs} = \pi(r_o^2-r_i^2) \text{ .}$$

So, for the vapor flow,

$$\frac{dP_v}{dx} = - \frac{8\mu_v \dot{m}_v(x)}{\rho_v \pi (r_o^2+r_i^2-2r_{lm}^2)(r_o^2-r_i^2)} \qquad (2a)$$

In this development, it has been assumed that the lateral mass flow rate due to evaporation and condensation does not significantly affect the annular vapor velocity profile. This approach is substantiated by Busse [6] who has found that the net pressure drop in the vapor over the entire length of a heat pipe is the same as for Poiseuille flow.

Heat is conducted axially by the following processes:

1. Heat is transferred from the pipe to the liquid in the evaporator, raising the internal energy of the liquid and causing evaporation.

2. Energy is transported axially as the vapor is convected to the condenser end.

3. At the condenser, the energy is released by condensation and conducted to the coolant.

For uniform heat addition in the evaporator, the mass rate of flow of vapor at an axial distance x from the evaporator end is given by

$$\dot{m}_v(x) = \frac{x\, Q_e}{L_e H} \quad , \qquad 0 \leq x \leq L_e$$

Similarly, in the condenser section (3)

$$\dot{m}_v(x) = \frac{L_t - x}{L_t - L_e} \cdot \frac{Q_e}{H} \quad , \qquad L_e \leq x \leq L_t$$

Combining equations (2a) and (3), integrating from 0 to L_t, and applying the result to the geometry of the vapor space,

$$P_{ve} - P_{vcd} = \frac{4 Q_e \mu_v L_t}{\pi \rho_v H (r_g^2 + r_{wo}^2 - 2r_{vlm}^2)(r_g^2 - r_{wo}^2)} \tag{4}$$

The third term in equation (1) represents the change in liquid pressure from the condenser to the evaporator. For annular flow through a porous media [7],

$$\frac{dP_l}{dx} = - K_1 \frac{\mu_l \dot{m}_l}{\rho_l A_{cs}} \tag{5}$$

where the wick cross-sectional flow area, $A_{cs} = \pi (r_{wo}^2 - r_{wi}^2)$. K_1 is a constant of proportionality, dimensions $(\text{length})^{-2}$ and is directly related to the frictional characteristics of the wick. As before, the assumption has been made that the lateral mass flow rate does not significantly affect the annular liquid velocity profile.

Again, for constant heat addition and removal in the evaporator and condenser, respectively,

$$\dot{m}_l(x) = \dot{m}_v(x) = \frac{x\, Q_e}{L_e H} \quad , \qquad 0 \leq x \leq L_e$$

(6)

$$\dot{m}_l(x) = \dot{m}_v(x) = \frac{L_t - x}{L_t - L_e} \cdot \frac{Q_e}{H} \quad , \qquad L_e \leq x \leq L_t$$

Combining equations (5) and (6), integrating from 0 to L_t, and applying the result to the geometry of the wick,

$$P_{lcd}-P_{le} = K_1 \frac{\mu_l Q_e L_t}{\rho_l H 2\pi (r_{wo}^2-r_{wi}^2)} \qquad (7)$$

The second and fourth terms in equation (1) represent the pressure difference across the menisci at the liquid-vapor interface in the condenser and the evaporator, respectively. These terms may be evaluated by taking a force balance on a meniscus as in Figure 3.

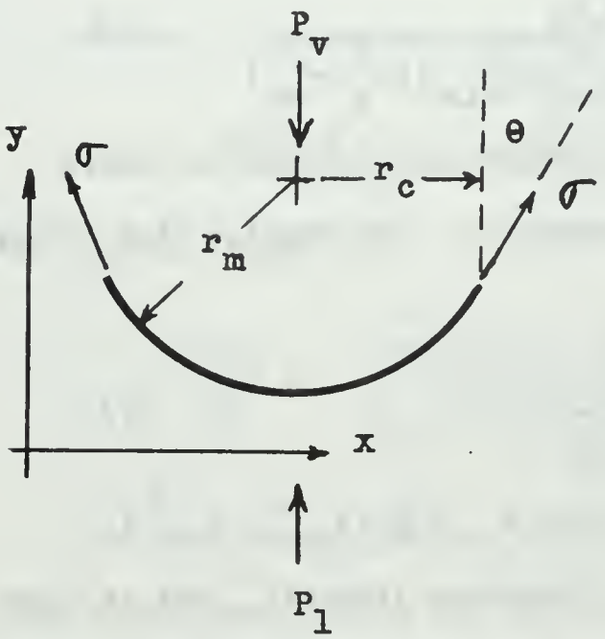

$$\Sigma F_y = 0 :$$

$$-(P_v-P_l)\pi r_c^2+\sigma 2\pi r_c \cos\theta = 0$$

or

$$P_v-P_l = \frac{2\sigma\cos\theta}{r_c}$$

Figure 3. Liquid Meniscus

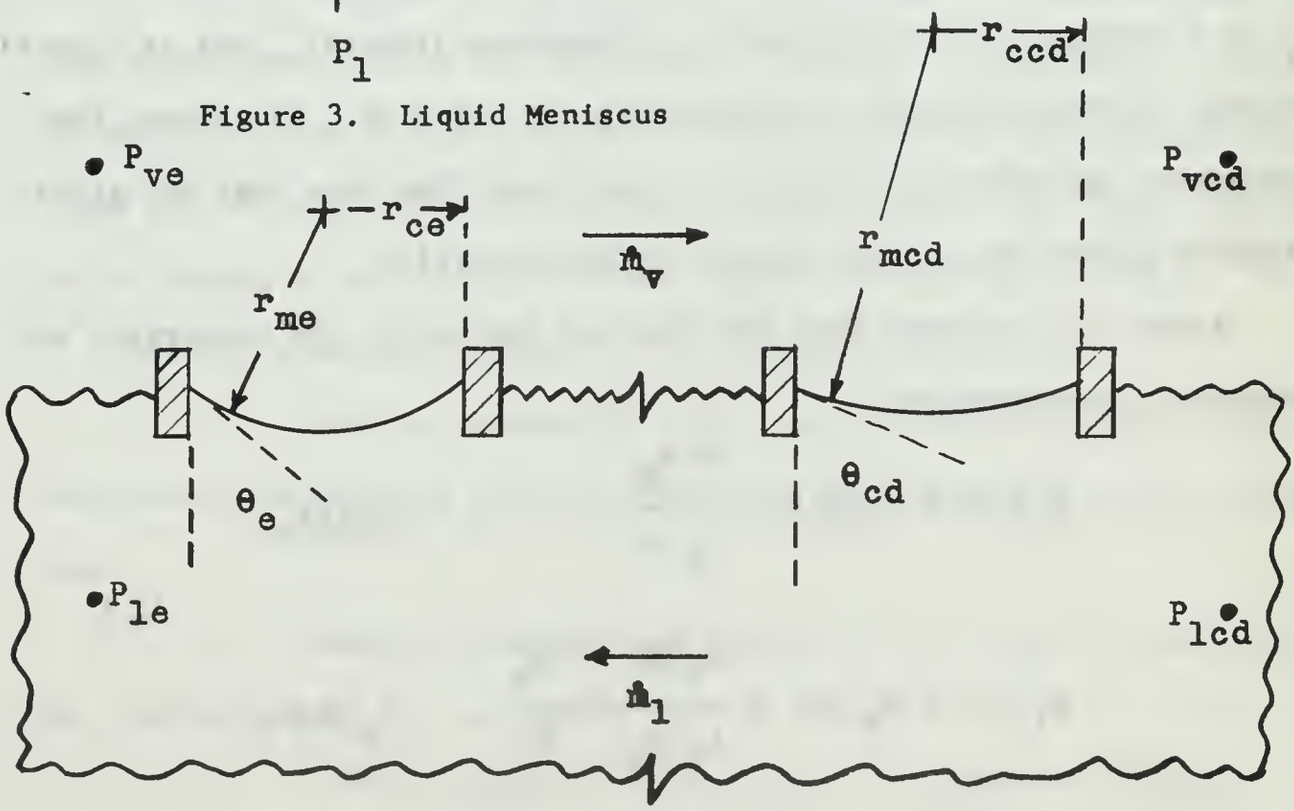

Figure 4. Schematic of the Liquid-Vapor Interface in a Heat Pipe Wick

Applied to Figure 4 at the condenser and evaporator, these terms become

$$P_{vcd}-P_{lcd} = \frac{2\sigma \cos\theta_{cd}}{r_{ccd}} \tag{8}$$

$$P_{le}-P_{ve} = -\frac{2\sigma \cos\theta_{e}}{r_{ce}}$$

where θ is now an effective contact angle [Appendix B].

Equation (1) may now be written in the form

$$\frac{4Q_e \mu_v L_t}{\pi \rho_v H(r_g^2+r_{wo}^2-2r_{vlm}^2)(r_g^2-r_{wo}^2)} + \frac{2\sigma \cos\theta_{cd}}{r_{ccd}} + \frac{K_1 \mu_l Q_e L_t}{\rho_l H 2\pi (r_{wo}^2-r_{wi}^2)}$$

$$- \frac{2\sigma \cos\theta_{e}}{r_{ce}} = 0 \tag{9}$$

At this point, a look at the relative magnitudes of the terms in equation (9) leads to some simplification. The second, third and fourth terms are of the same order of magnitude. The first and third terms may be compared simply by a look at their ratio.

$$\frac{\Delta P_v}{\Delta P_l} = \frac{8 \rho_l \mu_v (r_{wo}^2-r_{wi}^2)}{K_1 \rho_v \mu_l (r_g^2+r_{wo}^2-2r_{vlm}^2)(r_g^2-r_{wo}^2)} \tag{10}$$

By substituting in some representative values and assuming that $K_1 > 10^4$, it can be seen that for the apparatus and fluid used in this experiment, the maximum value this ratio can take is $\simeq 4 \times 10^{-4}$ [Appendix A]. It is therefore reasonable to neglect the effects of the change of vapor pressure.

Equation (9) now becomes

$$\frac{2\sigma \cos\theta_{cd}}{r_{ccd}} + \frac{K_1 \mu_1 Q_e L_t}{H \rho_1 2\pi (r_{wo}^2 - r_{wi}^2)} - \frac{2\sigma \cos\theta_e}{r_{ce}} = 0 \qquad (11)$$

or

$$K_1 \frac{\mu_1 Q_e L_t}{\rho_1 H 2\pi (r_{wo}^2 - r_{wi}^2)} = 2\sigma \left[\frac{\cos\theta_e}{r_{ce}} - \frac{\cos\theta_{cd}}{r_{ccd}} \right] \qquad (11a)$$

The left-hand term represents the pressure loss in the wick, while the right-hand term represents a pumping force due to capillary action at the vapor-liquid interface. Since the pressure loss is a positive value, the pumping force must be an equal positive value to offset the pressure loss.

A more specific interpretation of equation (11a) is that capillary action at the liquid-vapor interface provides the mechanism for moving the heat-transporting fluid medium. This mechanism will be explored next in Part C of Heat Pipe Theory, Wick Operation.

C. WICK OPERATION

1. Capillary Radius

The theoretical terms which describe liquid motion in the wick are related by equation (11a),

$$K_1 \frac{\mu_1 Q_e L_t}{\rho_1 H 2\pi (r_{wo}^2 - r_{wi}^2)} = 2\sigma \left[\frac{\cos\theta_e}{r_{ce}} - \frac{\cos\theta_{cd}}{r_{ccd}} \right] \qquad (11a)$$

From equations (3) and (6),

$$Q_e = H \dot{m}_{lt} \qquad (12)$$

Substituting equation (12) into equation (11a),

$$K_1 \frac{\mu_l L_t \dot{m}_{lt}}{\rho_l \pi (r_{wo}^2 - r_{wi}^2)} = 2\sigma \left[\frac{\text{Cos}\theta_e}{r_{ce}} - \frac{\text{Cos}\theta_{cd}}{r_{ccd}} \right] \quad (13)$$

The right-hand term of equation (11a) represents the pressure change across the menisci of the liquid-vapor interface, while the left-hand term represents the pressure change in the fluid passing through the wick. Symbolically,

$$\Delta P_l = \Delta P_{pp} \quad (14)$$

Equation (12) shows that the choice of a fluid medium reduces the problem of maximizing Q_e to that of maximizing $\dot{m}_{lt}$. The choice of dimensions for the wick further reduces the problem of maximizing $\dot{m}_{lt}$. Solving equation (13) for $\dot{m}_{lt}$,

$$\dot{m}_{lt} = \frac{2\sigma \rho_l}{\mu_l} \frac{\pi (r_{wo}^2 - r_{wi}^2)}{L_t} \frac{1}{K_1} \left[\frac{\text{Cos}\theta_e}{r_{ce}} - \frac{\text{Cos}\theta_{cd}}{r_{ccd}} \right] \quad (15)$$

The term $\frac{2\sigma \rho_l}{\mu_l}$ is a function of the properties of the fluid medium.

The term $\frac{\pi (r_{wo}^2 - r_{wi}^2)}{L_t}$ is a function of the dimensions of the pipe and wick. For the present, these terms will be considered constant.

So,

$$\dot{m}_{lt} = C \frac{1}{K_1} \left[\frac{\text{Cos}\theta_e}{r_{ce}} - \frac{\text{Cos}\theta_{cd}}{r_{ccd}} \right] \quad (15a)$$

The remaining terms are functions of the internal characteristics of the wick and of the wick-liquid wetting angle. More specifically, K_1 is related to the internal frictional characteristics of the wick, and the term in brackets is a function of the capillary interaction between

the wick and the fluid medium. A detailed look at each of these terms provides a more fundamental view of the individual mechanisms.

In a uniform, annular wire mesh wick, there are two characteristic capillary radii: r_{cpp}, the radial capillary pumping radius, and r_{cf}, the axial capillary frictional radius. The radial capillary pumping radius is related to the space opening between wires in the mesh. The axial capillary frictional radius is related to the manner in which adjacent layers are stacked and to the type of mesh weave, a consideration which is reflected in the stacking factor. The stacking factor describes the physical contact relationship of tightly-wound, adjacent layers in the wick. The friction factor, K_1, is inversely related to the square of the capillary frictional radius [2],

$$K_1 \propto \frac{1}{r_{cf}^2} \tag{16}$$

Relationship (16) shows that the resistance to flow approaches a minimum as the capillary radius approaches a maximum. The capillary pumping term is shown by equation (11a) to be inversely related to the first power of the capillary pumping radius. If $r_{ce} = r_{ccd} = r_{cpp}$,

$$\dot{m}_{lt} \propto \frac{1}{(1/r_{cf})^2} \frac{1}{r_{cpp}} \left[\text{Cos}\theta_e - \text{Cos}\theta_{cd} \right] \tag{17}$$

Considering, for the moment, that the wetting angles are unequal constants, then,

$$\dot{m}_{lt} \propto \frac{1}{(1/r_{cf})^2} \cdot \frac{1}{r_{cpp}} \tag{17a}$$

Equation (17a) shows that for constant unequal wetting angles $\dot{m}_{lt}$ is dependent upon two factors:

1. Pumping Force $\propto 1/r_{cpp}$
2. Frictional Force $\propto 1/r_{cf}^2$

As long as the wick performs its basic functions of holding the liquid and providing capillary pumping at the liquid-vapor interface, $\dot{m}_{lt}$ can be improved by increasing r_{cf} and decreasing r_{cpp}. The next step, then, is to find the limits of r_{cpp} and r_{cf} within which the wick continues to perform its functions.

Only the upper limit of r_{cf} is of interest, since $\dot{m}_{lt}$ is improved by increasing r_{cf}. Since r_{cf} does not affect the capillary pumping action, its only required function is that of holding the liquid in the wick, if the wick ends are not sealed. Considering the conditions under which the wick performs, the mechanics that hold the liquid in the wick may be idealized. The following figure is an end section of the wick, and the two menisci shown represent any two menisci separated by vertical height ht.

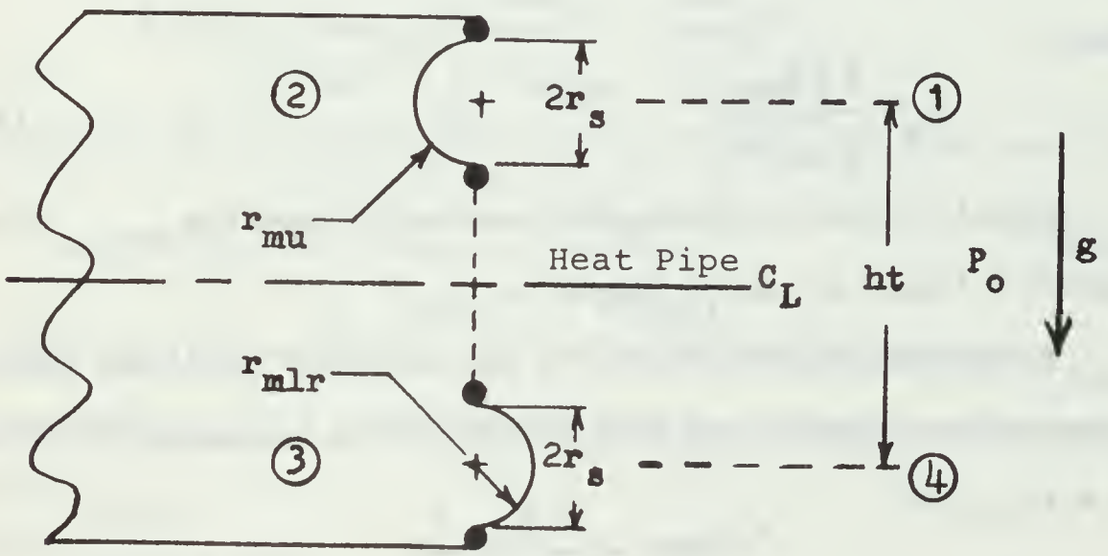

The limiting maximum value of r_{mu} and r_{mlr} is equal to $r_{spacing}$ [Appendix B]. This limiting condition occurs when ht is the maximum height of fluid the capillary action will support. Taking the sum of pressure differences from ① to ④ equal to zero,

$$\Delta P_{1-4} = (P_1 - P_2) + (P_2 - P_3) + (P_3 - P_4) + (P_4 - P_1) = 0 \qquad (18)$$

where $P_1 = P_4 = P_o$

$$P_1 - P_2 = \frac{2\sigma}{r_{mu}} = \frac{2\sigma}{r_s}$$

$$P_2 - P_3 = \frac{-\rho g\ ht}{g_o}$$

$$P_3 - P_4 = \frac{2\sigma}{r_{mlr}} = \frac{2\sigma}{r_s}$$

Equation (18) now becomes

$$\frac{2\sigma}{r_s} - \frac{\rho g\ ht}{g_o} + \frac{2\sigma}{r_s} = 0 \qquad (18a)$$

or,

$$r_s = \frac{4\sigma g_o}{\rho g\ ht} \qquad (18b)$$

Equation (18b) represents the maximum allowable $r_{spacing}$ that will support a liquid column of height ht.

In applying equation (18b) to the capillary frictional radius, a conservative error of less than two percent is introduced by letting $ht = 2r_{wo}$. So,

$$r_{cfmax} \simeq \frac{\sigma g_o}{\rho g} \cdot \frac{2}{r_{wo}} \qquad (19)$$

Applying (18b) to the capillary pumping radius, this becomes

$$r_{cppmax} = \frac{4\sigma g_o}{\rho g\ ht} = \frac{\sigma g_o}{\rho g} \cdot \frac{2}{r_{wo}} \qquad (20)$$

Equations (19) and (20) are the maximum capillary radii that will hold fluid in an annular wick of outside diameter 2 r_{wo}, horizontally oriented to the gravitational field. Therefore, $\dot{m}_{lt}$ can be increased by increasing r_{cf} to its maximum limit set by equation (19). At the same time, r_{cpp} must not exceed the limiting value established by equation (20). Note that if the wick ends are sealed, equation (19) does not apply and there is no restriction on r_{cf} with regard to fluid holding ability.

By separating r_{cpp} into r_{cppe} and r_{cppcd}, other improvements can be gained. Recalling equation (15a)

$$\dot{m}_{lt} = C \frac{1}{K_1} \left[\frac{\cos\theta_e}{r_{ce}} - \frac{\cos\theta_{cd}}{r_{ccd}} \right] \qquad (15a)$$

and using the definitions above, rewrite equation (15a).

$$\dot{m}_{lt} \propto \frac{1}{(1/r_{cf})^2} \left[\frac{\cos\theta_e}{r_{cppe}} - \frac{\cos\theta_{cd}}{r_{cppcd}} \right] \qquad (15b)$$

Consider for the moment that r_{cf}, θ_e, and θ_{cd} are constants, then

$$\dot{m}_{lt} \propto \left[\frac{C_1}{r_{cppe}} - \frac{C_2}{r_{cppcd}} \right] \qquad (15c)$$

Relation (15c) shows that $\dot{m}_{lt}$ can be improved by decreasing r_{cppe} and increasing r_{cppcd}. Equation (20) however, establishes the upper limit on r_{cppcd}.

2. Wetting Angle

Refer again to equation (15b).

$$\dot{m}_{lt} \propto \frac{1}{(1/r_{cf})^2} \left[\frac{\cos\theta_e}{r_{cppe}} - \frac{\cos\theta_{cd}}{r_{cppcd}} \right] \qquad (15b)$$

Consider for the moment that r_{cf}, r_{cppe}, and r_{cppcd} are constants. Then,

$$\dot{m}_{lt} \propto \left[\frac{\cos\theta_e}{C_3} - \frac{\cos\theta_{cd}}{C_4} \right] \qquad (15d)$$

Equation (15d) shows that $\dot{m}_{lt}$ will be improved as

$$\theta_e \longrightarrow 0°$$
$$\theta_{cd} \longrightarrow 180°$$

3. Summary

It has been shown that five separate and independent parameters may be adjusted to improve $\dot{m}_{lt}$:

Adjustment/Parameter	Limits	
Increase r_{cf}, the capillary frictional radius	$\max = \frac{\sigma g_o}{\rho g} \frac{2}{r_{wo}}$	, min = N.A.
Increase r_{cppcd}, the condenser capillary pumping radius	$\max = \frac{\sigma g_o}{\rho g} \frac{2}{r_{wo}}$	, min > r_{cppe}
Decrease r_{cppe}, the evaporator capillary pumping radius	max < r_{cppcd}	, min > 0
Decrease θ_e, the evaporator wetting angle	max < θ_{cd}	, min = 0
Increase θ_{cd}, the condenser wetting angle	max = 90°	, min ≥ θ_e

Note that this entire development disregarded the change in pressure in the vapor, shown to be negligible by equation (10). By greatly increasing r_{cf}, K_1 may be reduced to the magnitude at which $\triangle P_v$ is no longer negligible. In such case, $\triangle P_v$ is important in the operation of the pipe, but no changes within the wick will have a direct bearing upon $\triangle P_v$. Only as $\dot{m}_{vt}$ is affected by increasing $\dot{m}_{lt}$ will $\triangle P_v$ be

indirectly affected, as shown by equation (4). Even with these considerations, the statements summarized above are still valid.

Also, note that the maximum attainable θ_{cd} is 90°. Since any larger contact angle would imply that $P_{vcd} < P_{lcd}$, and since the vapor cannot condense if that condition exists, the pipe cannot operate if $\theta_{cd} > 90°$.

The minimum limit on r_{cppcd} and the maximum limit on r_{cppe} are established by equation (15b), which shows that if the wetting angles are equal, the pipe will operate only as long as $r_{cppe} < r_{cppcd}$.

D. RADIAL HEAT TRANSFER

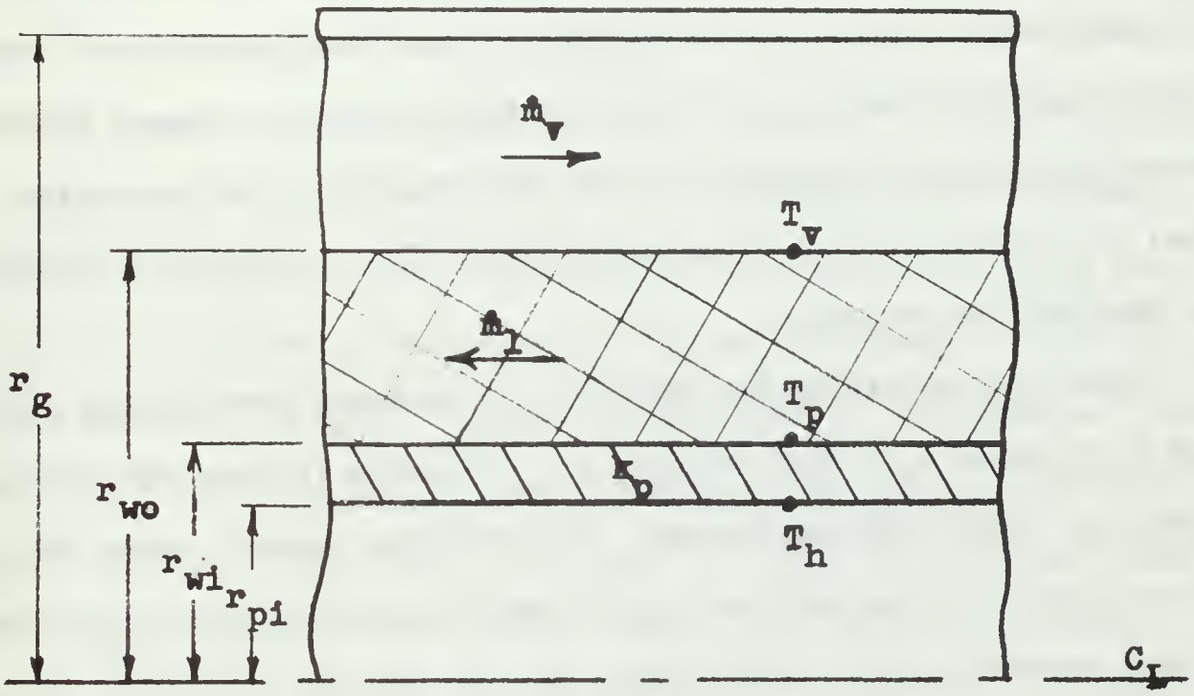

Figure 5. Radial Heat Transfer in the Evaporator

For radial heat transfer in an annular geometry such as Figure 5 [8],

$$\frac{Q}{L} = \frac{2\pi(T_v - T_h)}{\frac{\ln(r_{wi}/r_{pi})}{k_p} + \frac{\ln(r_{wo}/r_{wi})}{k_w}} \qquad (21)$$

The electrical analogy may be used to represent the above equation:

$$\frac{Q}{L} \longrightarrow 2\,T_v \;\; \underset{\frac{\ln(r_{wo}/r_{wi})}{k_w}}{\sim\!\sim} \;\; 2\,T_{po} \;\; \underset{\frac{\ln(r_{wi}/r_{pi})}{k_p}}{\sim\!\sim} \;\; 2\,T_h$$

Since k_w is some function of k_l and k_{wire},

$$k_l \leq k_w < k_{wire}$$

From the sketch above, it can be seen that for the wick,

$$\frac{Q}{L} = \frac{-2\pi (T_v - T_{po})\, k_w}{\ln(r_{wo}/r_{wi})} \qquad (22)$$

Equation (22) shows that, for a constant $\frac{Q}{L}$, a lower value of k_w requires a larger value for $T_{po} - T_v$. A greater ΔT across the wick is accompanied by a greater chance of boiling in the wick or at the pipe wall. The consequences of boiling within the wick structure could be disastrous. If the r_{cpp} of the wick is less than the radius of the bubbles caused by boiling, the bubbles probably will be trapped within the wick structure, resulting in both the formation of an insulating layer of vapor and in the reduction of fluid flow. Either will reduce the desired flow of heat.

These considerations are particularly important when efforts are made to increase r_{cf}. Any increase in r_{cf} results in less wick material within the fluid-wick combination. The effective thermal conductivity of the fluid-wick combination, k_w, is some function of the relative amounts of each present, but it also depends upon the physical continuity of the pipe and wick material in the radial direction. Accordingly, it is possible to increase r_{cf} to the point that k_w is sufficiently lowered to cause boiling.

There are relationships available for estimating k_w, $\Delta T_{boiling}$, and the radius of bubbles produced [3], [9]. The relationship for k_w involves such gross approximations that accurate predictions are virtually impossible. However, it is important to recognize that this situation will probably dictate the practical upper limit for r_{cf}, rather than the limit established by equation (19).

III. DESCRIPTION OF EQUIPMENT

The equipment used in this study was basically the same apparatus and auxiliary equipment designed by W. L. Mosteller [3] and subsequently used by H. E. Kilmartin [4] in his investigation. The heat pipe was everted (inside out), with the heater and condenser placed on the inside of the pipe. The wick was wrapped around the pipe in an annular shape. An enclosing glass envelope around the entire apparatus served as the vapor space container and facilitated visual observation of heat pipe operation. Figure 6 is a sectional view of the everted heat pipe, and Figure 7 is a photograph of the apparatus.

The actual pipe was an eighteen -inch length of .750 inch O.D., type "A" nickel, cold-drawn seamless tube with a .065 inch wall thickness. The working length was fourteen inches, with a welded metal plug and a one-half inch section of asbestos (serving as the adiabatic section) separating the 4-3/4 inch evaporator from the 8-3/4 inch condenser section. The evaporator function was performed by an electric cartridge heater, rated at 1,000 watts, wrapped in one layer of brass shim stock tinned to the cartridge. The heater was pressed into the evaporator section to ensure good physical contact with the inside of the pipe, thereby providing an even temperature distribution to the entire evaporator. The heater cartridge, being 3.9 inches long, provided an evaporator surface area of 9.18 square inches at the pipe surface. Power to the heater was controlled by a variac and measured by an AC wattmeter. Cooling water to the condenser entered through the center tube of a return-flow annular design, collecting heat from the pipe as it passed back through the outer annulus. The flow rate was monitored by use of a precision bore flowrator.

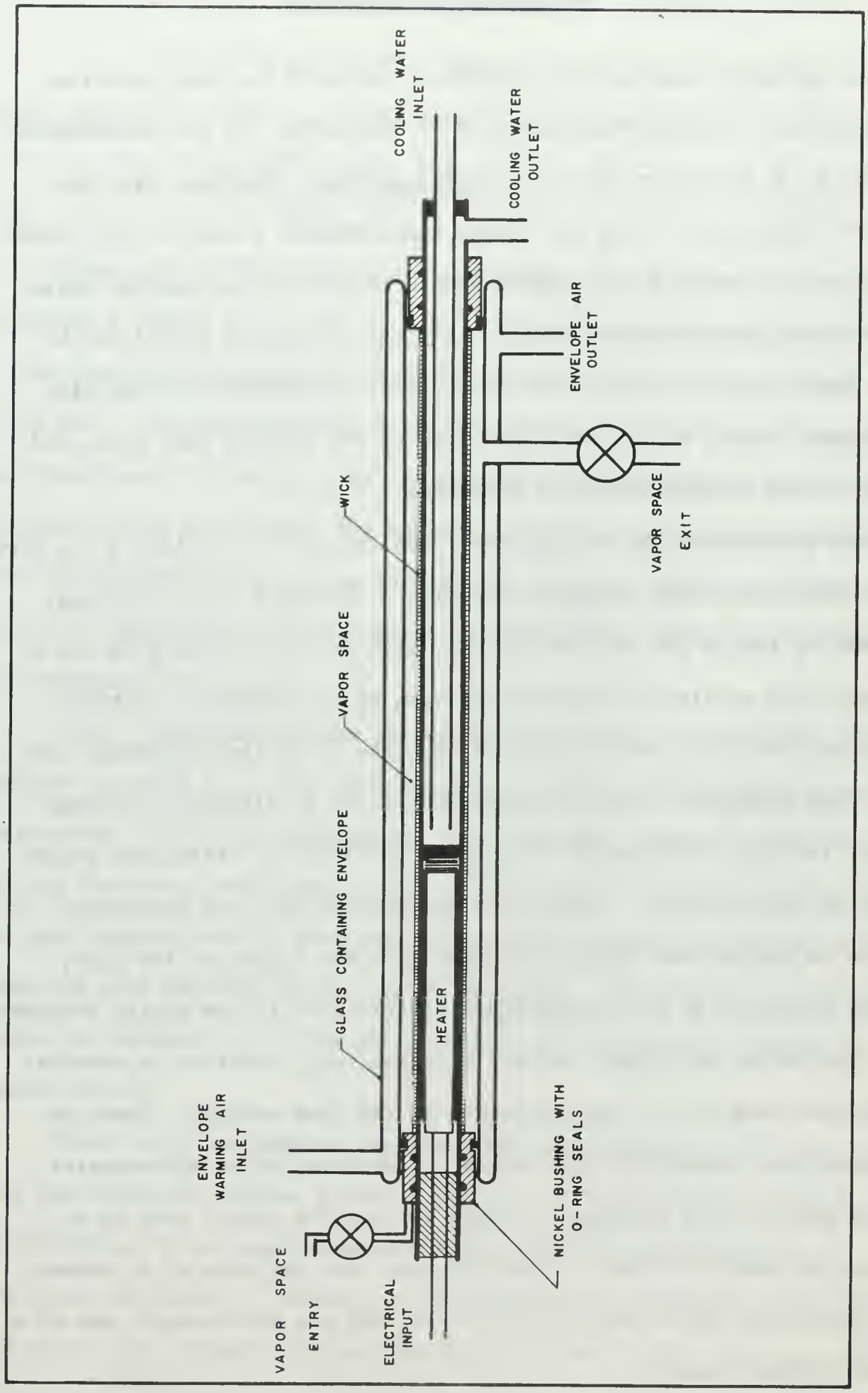

Figure 6. Sectional View of Everted Heat Pipe

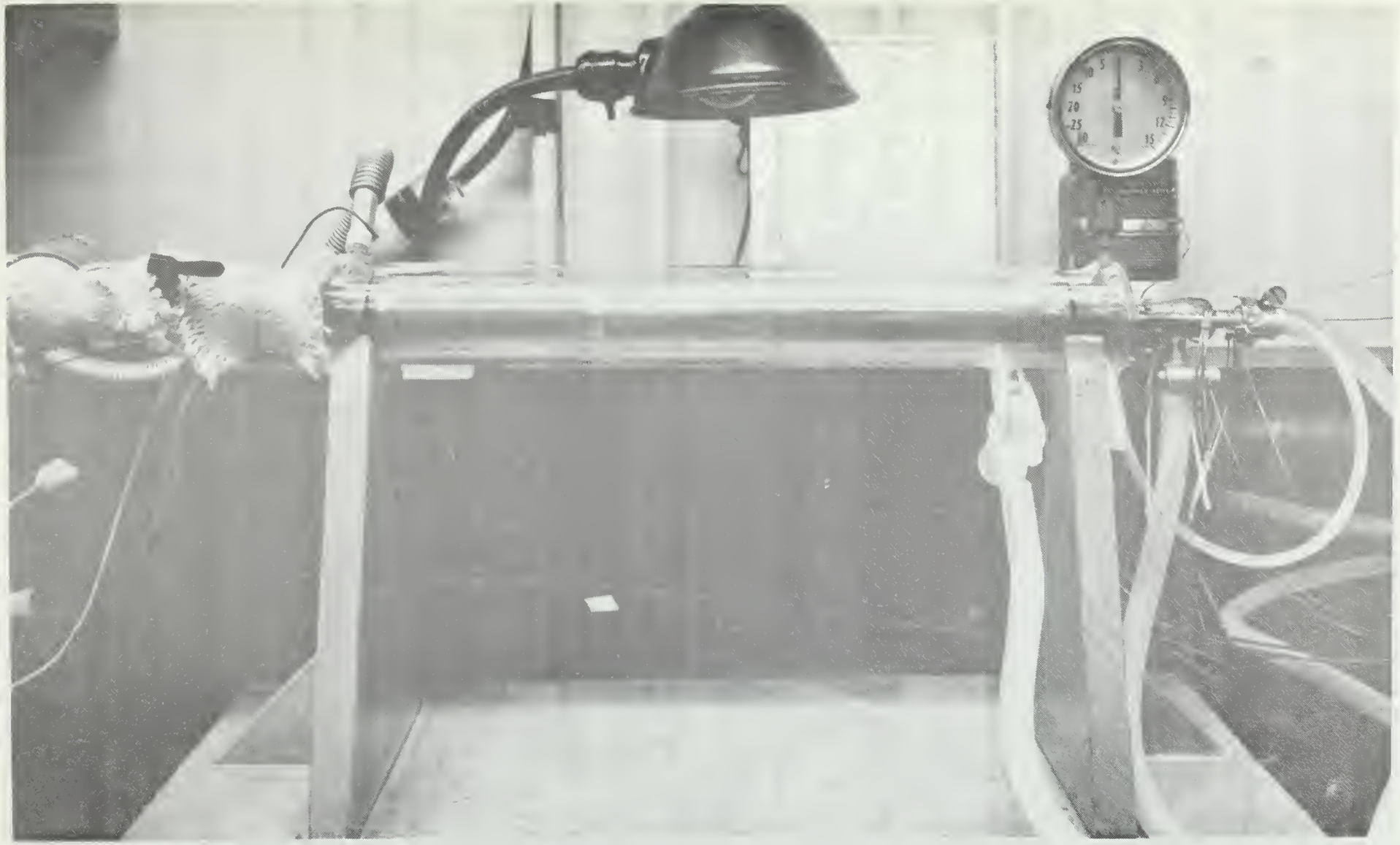

Figure 7. Photograph of Everted Heat Pipe

An annular glass envelope, constructed from two heat-resistant glass tubes closed at the ends, enclosed the pipe. The 1.31 inch I.D. of the inner tube enclosed the vapor space and provided the visual observation function mentioned above. The second tube enclosed the first, leaving a .16-inch radial annular space. This annular space was connected to an oil-free, heated air supply which was kept at, or a few degrees above, the temperature in the vapor space. The variac-controlled, heated air supply to the annular space served two purposes - one, to heat the inner tube to prevent the formation of view-blocking condensation and, secondly, to provide a negligible radial temperature gradient at the inner tube so that heat losses to the environment would be negligible. The glass envelope was sealed to the pipe at each end by rubber "O"-rings mounted on insulated bushings of the same nickel as that in the pipe. This arrangement allowed visual observation of the heat pipe operation while ensuring that the power input of the heater was the only source of heat and that all the heat generated by the heater was removed by the condenser. Pressure in the vapor space was measured by a bourdon vacuum-pressure gage.

Temperature measurements were taken throughout by thermocouples. All thermocouples were led to an insulated box containing a thermocouple selector switch and a multi-connector plug. Readings in millivolts were taken with a Hewlett-Packard 2010 Data Acquisition System, which included an integrating digital voltmeter and a guarded data amplifier.

To measure temperatures in the pipe, five .041-inch O.D. type-T, copper-constantan, metallic-sheathed thermocouples were placed in milled grooves in the pipe and covered by silver solder. The pipe was then filed down to approximately its original dimensions. For the vapor space, one

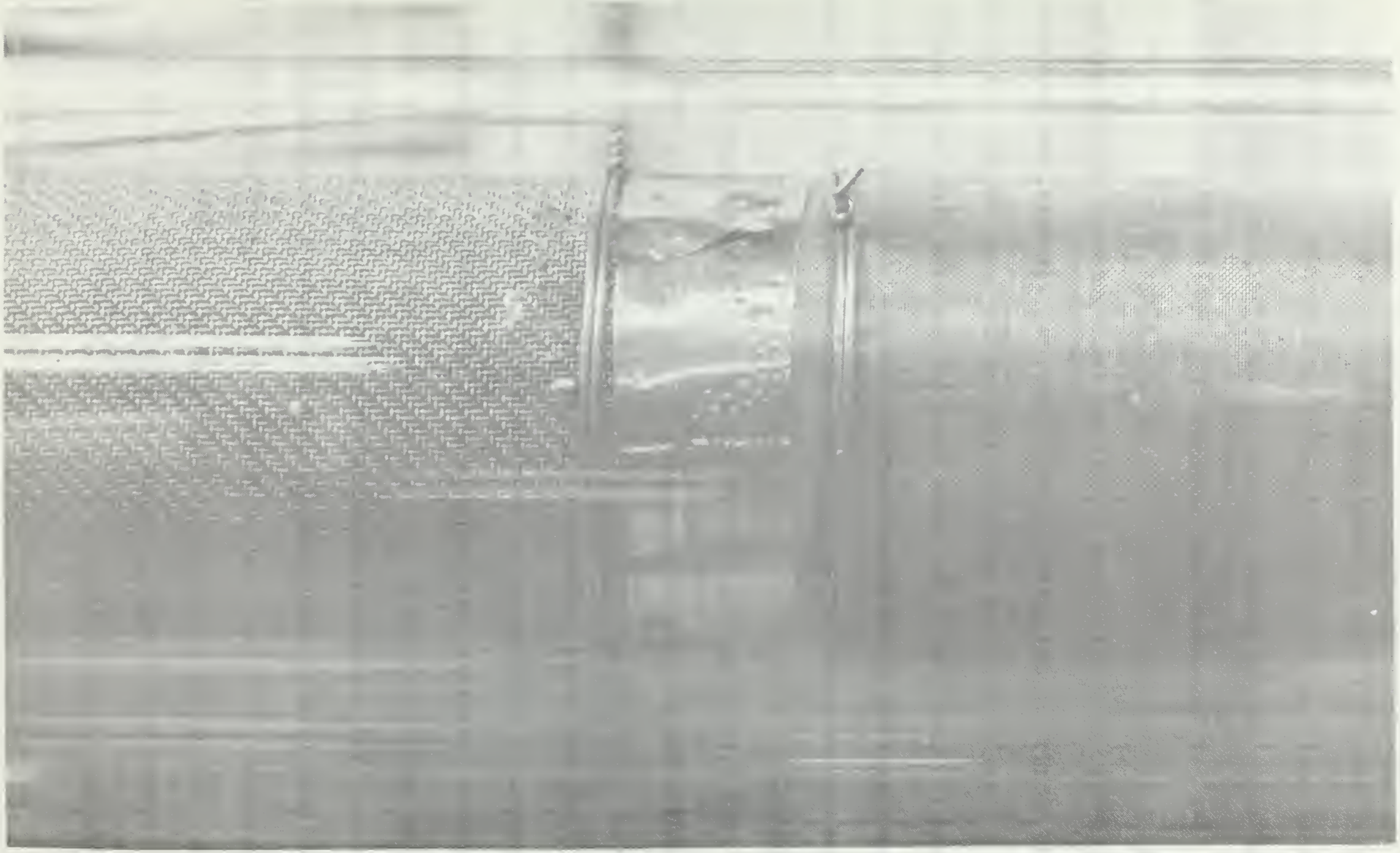

Figure 8. Photograph of Wick Installation

.040 inch O.D. thermocouple of the same type described above was inserted through Conax fittings in each bushing and adjusted to the desired longitudinal position. Other thermocouples were used in the condenser cooling water inlet and the heated annular space in the glass envelope.

The filling and purging apparatus was constructed from a 1,000 ml pyrex flask and three teflon "O"-ring type glass valves. A valved filling spout was added to the top of the flask while valved outlets were added at the top and bottom of the flask, respectively, and connected via a glass tube at the discharge side of the lower outlet. This common connection then led to the vapor space of the heat pipe via a toggle valve installed in the evaporator end bushing. An outlet from the vapor space was installed through the glass envelope and valved with a glass stopcock.

The basic wick consisted of a plain weave 80 mesh nickel wire cloth. The cloth was cut into a rectangle 14 by 13 inches, and cleaned by the improved cleaning method (See Appendix C). One edge was spot-welded to the pipe, the cloth was wrapped tightly around the pipe, and spot-welded in place. A changeable top layer was cut in two at the evaporator-condenser interface, wrapped around the basic mesh, spot-welded in place, and secured by two wraps of 20 mil chromel wire at the end of each subsection. The evaporator-condenser interface and each end of the top layer were wrapped securely with spot-welded strips of stainless steel shim stock. This installation resulted in a .1 inch thick wick. Figure 8 is a photograph of the wick installation on the pipe.

Figure 9 is a diagram of the entire system and Figure 10 is a photograph of the system.

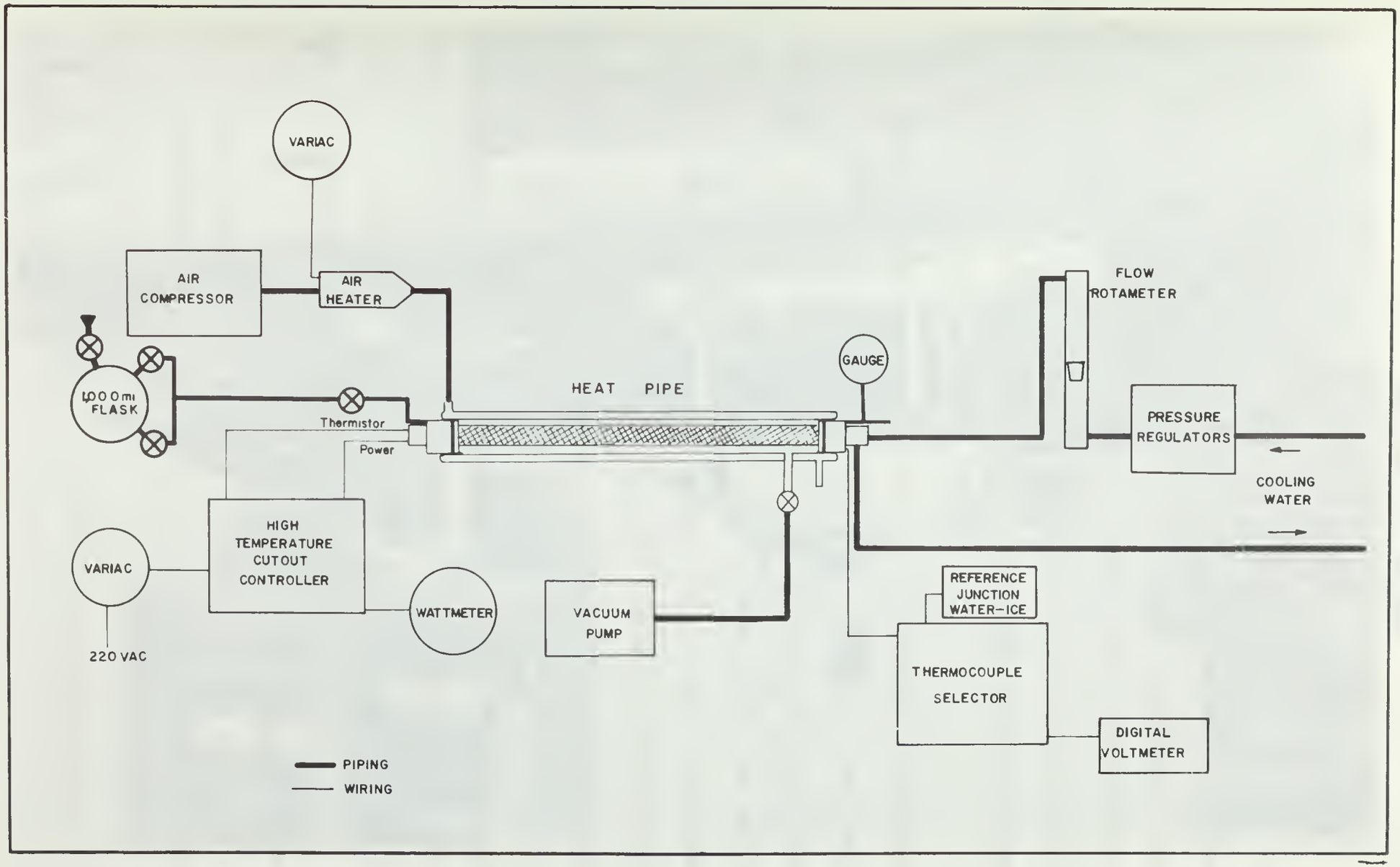

Figure 9. Block Diagram of Heat Pipe Apparatus

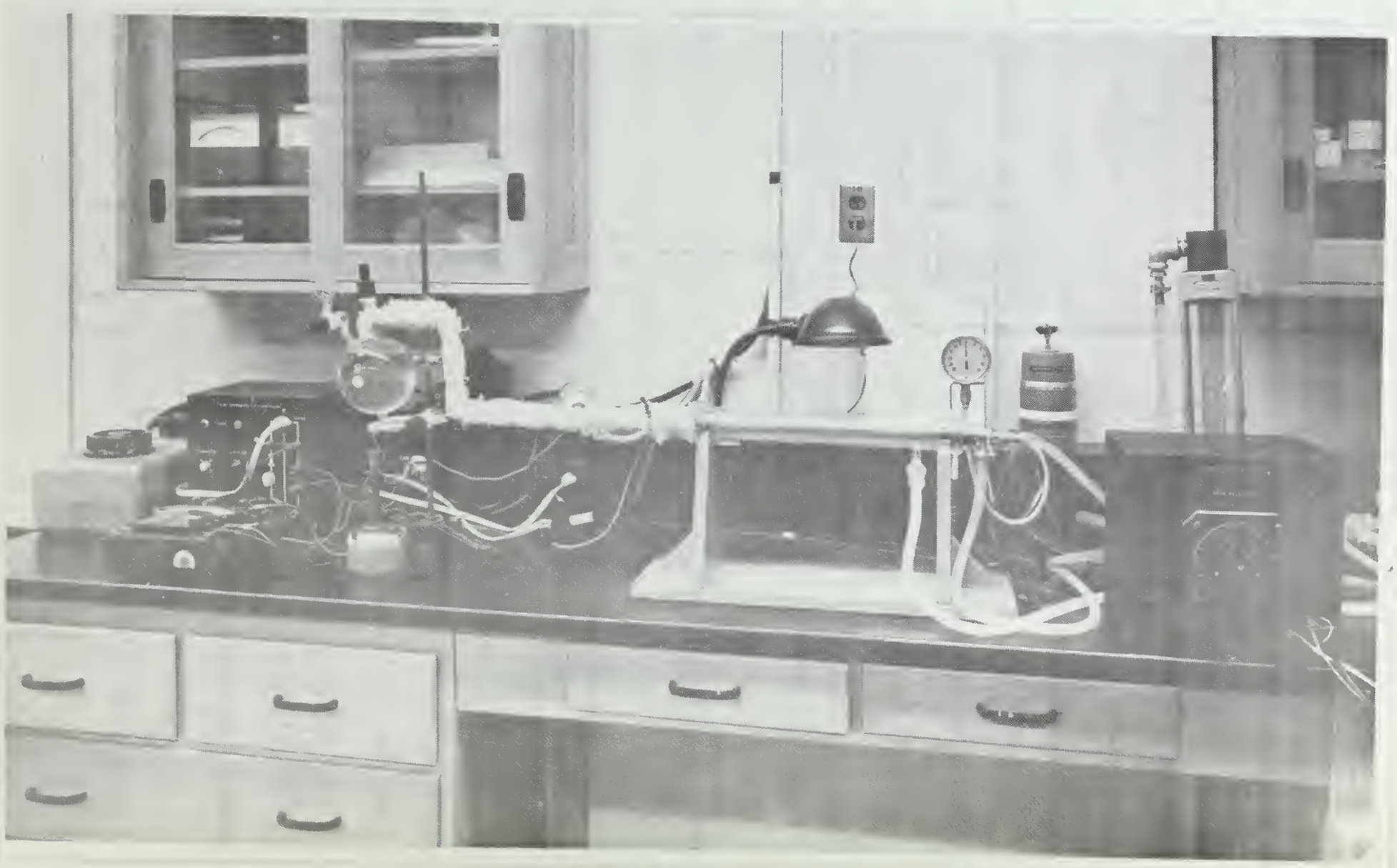

Figure 10. Photograph of Experimental Apparatus

IV. EXPERIMENTAL PROCEDURE

A. FILLING AND PURGING

There are two primary considerations in filling the wick. First, Kunz et al [10] have stated that the presence of non-condensable gases in the working fluid leads to an increase in the wick friction factor. They hypothesize that non-condensable bubbles can be trapped within the wick and serve to restrict the flow of liquid, hence lowering the pipe performance. Investigations by Ginwala et al [11] tend to substantiate this view.

Second, it is desirable to fill the wick completely with the working fluid so that all parts of the wick will participate in the fluid pumping mechanism. Any section of the wick not filled with fluid will serve to lower the performance of the pipe. An air "hole" within the wick restricts the flow of the fluid and restricts the radial flow of heat. Additionally, for this particular experiment it was absolutely necessary that the top layer be filled at all times in order that the changes made only in the top layer be shown effective.

Accordingly, an effort was made to remove non-condensables from the working fluid and to purge the heat pipe of non-condensables prior to filling the wick. The purging and filling apparatus was used to accomplish both desirable ends. The steps used were as follows:

1. Using the heated air envelope, heat the entire pipe to two or three degrees above 212°F.

2. Fill the 1,000 ml flask with about 750 ml of distilled water and close the fill valve.

3. With the lower flask valve closed, the upper flask valve open, the vapor space entry valve open, and the vapor space exit valve open, evacuate all air from the pipe and filling apparatus with a vacuum pump via the vapor space exit. Close the vapor space exit valve.

4. Light a bunsen burner under the 1,000 ml flask, let the pressure in the system build up to about 1 psig, then open the vapor space exit valve and allow the entire system to steam out at 1 psig while the distilled water boils for 15 minutes.

5. Rotate the pipe so that the vapor space exit valve is pointing upward. Open the lower valve on the 1,000 ml flask and fill the pipe completely with deaerated water. Maintain 1 psig.

6. Rotate the pipe so that the vapor space exit valve is pointing downward. Close the lower valve on the 1,000 ml flask and allow vapor at 1 psig to blow the vapor space of the pipe free of all water not absorbed by the wick.

7. Close the vapor space inlet and outlet valves. Set the heat input to 20 watts, turn on condenser cooling water, reduce the air envelope temperature, and allow the pipe to settle at that operating point.

It was found that this procedure resulted in a fairly high vacuum, about 29.8 inches Hg, in the vapor space at room temperature. Consequently, when runs were made on the apparatus filled in this manner, dryout was reached in only seven data steps. Kilmartin [4] and Mosteller [3] both had shown that dryout occurs at very low heat fluxes when operating at high vacuums, so a decision was made to operate at less vacuum (higher absolute pressure). This was accomplished by eliminating the use of the vacuum pump in step 3. This change resulted in the presence

of some additional non-condensables in the vapor space, a matter which was not expected to greatly inhibit pipe performance. Since the fluid had been purged of most non-condensables by boiling, and since the 15-minute steaming period should have purged most non-condensables from the vapor-space, it seemed likely that by eliminating the vacuum pump evacuation step, only a small increase in non-condensables would result. Furthermore, as stated by Mosteller [3], the condenser is over-designed, so it was expected that most non-condensables would be pushed into the condenser end vapor "dead space" and have no real effect on pipe performance. This step was taken and the pipe was found to operate between 27 and 24 inches Hg vacuum, and the dryout point was extended considerably.

It was then found that the pipe exhibited the strange behavior of producing non-repetitive data in succeeding runs on the same filling. This was deduced to be caused by the formation of vapor bubbles in the evaporator, so the procedure was modified again. After filling, and after each run, the pipe was allowed to cool to at least 100°F prior to beginning a new run. The vapor bubble formation will be discussed further in Discussion of Results.

B. PARAMETER CHANGES

In order to show the effect of each parameter discussed in the theoretical development, three different sizes of mesh and three different cleaning methods were used on the two sections of the changeable top layer of the wick. The three sizes - 50, 80, and 150 mesh were chosen to show the effect of changing r_{cppe} and r_{cppcd}. Recall that the remainder of the wick remained 80 mesh while only the top layer was changed. The effect of r_{cf} was to be shown by removing, successively, the two bottom layers of the basic wick, leaving a .25-inch length of

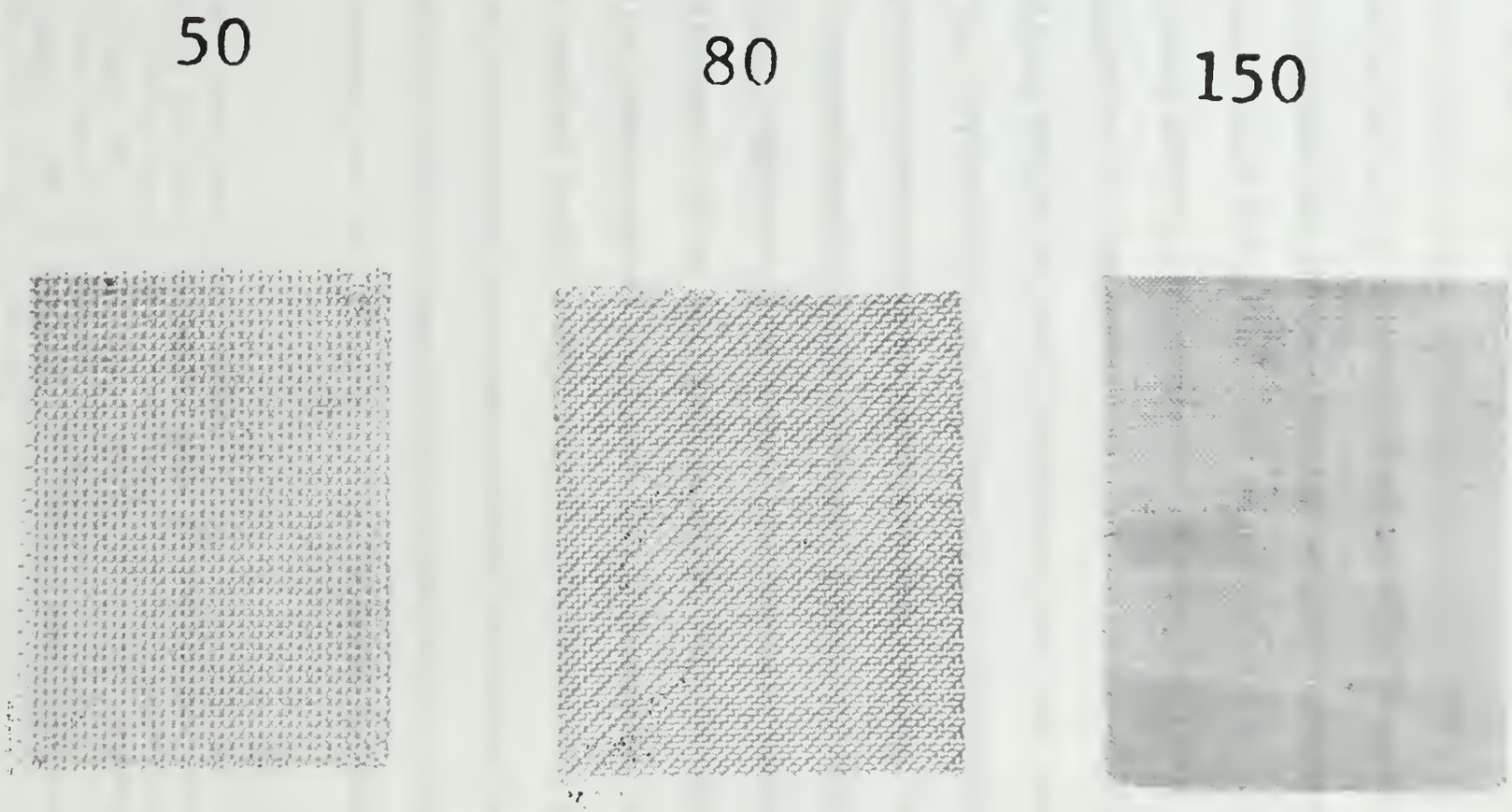

Figure 11. Photograph of Mesh Size Samples

each layer present at each end to create an annular passage within the wick. The three cleaning methods were used to show the effect of changing θ_e and θ_{cd}. The cleaning methods were named, in ascending order of expected effectiveness, the Standard (S), Improved (I), and Most Improved (M) methods. Appendix C outlines the procedure for each cleaning method. Figure 11 is a photograph of three samples of the mesh sizes used, and Table 1 lists pertinent data concerning the mesh sizes.

Three runs were made on each wick combination in accordance with the schedule shown in Table 2, except that runs on combination numbers 8-11 were not made. See Discussion of Results, Effect of Wick Aging.

TABLE 1

SUMMARY OF MESH CONSTANTS [4]

	50 Mesh	80 Mesh	150 Mesh
Wire Diameter (inches)	.009	.007	.0026
Stacking Factor	1.78	2.0	1.54
Porosity (percent)	64.4	55.2	68.2
Surface Open Area (percent)	35.3	19.4	37.4
Space Opening (inches)	.0134	.0055	.0041

TABLE 2

SUMMARY OF WICK COMBINATIONS

Wick Combination Number	Top Layer Combination		Shows Effect of
	Evaporator	Condenser	
1	80 (S)	80 (S)	Standard
2	150 (S)	80 (S)	r_{cppe}, the evaporator capillary pumping radius
3	50 (S)	80 (S)	r_{cppe}
4	80 (I)	80 (S)	θ_e, the evaporator wetting angle
5	80 (M)	80 (S)	θ_e
6	80 (S)	150 (S)	r_{cppcd}, the condenser capillary pumping radius
7	80 (S)	50 (S)	r_{cppcd}
8	80 (S)	80 (I)	θ_{cd}, the condenser wetting angle
9	80 (S)	80 (M)	θ_{cd}
10	80 (S)	80 (S)	r_{cf}, the capillary frictional radius
11	80 (S)	80 (S)	r_{cf}

NOTES:

1. Runs were conducted only on combination numbers 1-7.
2. Numbers in second and third column denote mesh size.
3. Letters in parentheses denote cleaning procedure: (S) - Standard; (I) - Improved; (M) - Most Improved.
4. Wick combination number 10 is with the bottom layer of the basic wick removed.
5. Wick combination number 11 is with the bottom two layers of the basic wick removed.

C. DATA TAKING

After the appropriate wick combination had been installed, the pipe was filled and allowed to cool to 100°F, the power to the evaporator heater was set at 20 watts, the condenser cooling water was set at maximum flow rate - 1.6 gallons/minute, the air envelope temperature was adjusted to show only a small ring of mist on the glass, and the pipe was allowed to settle at that operating point. When all temperatures had settled down, the following data were taken:

1. Three evaporator pipe surface temperatures
2. Two condenser pipe surface temperatures
3. One vapor space temperature
4. Vapor space pressure
5. Air envelope inlet temperature
6. Condenser cooling water inlet temperature
7. Power to the evaporator heater

The power was then increased 20 watts and the procedure was repeated by steps until a point was reached at which the evaporator temperatures would not settle down and had risen more than 1 millivolt (about 40°F) above those of the previous step. This point was defined as dryout for data taking purposes.

V. DISCUSSION OF RESULTS

A. FLUID FLOW RATE

The objective of this investigation included an experimental evaluation of wick performance under the influence of various changeable parameters. In particular, an indication of the relative values of fluid flow rate at dryout were of interest, since the theoretical development was oriented toward ways to increase the maximum $\dot{m}_{lt}$. Since an improving parameter change was expected to increase the maximum $\dot{m}_{lt}$, such change was expected to move the dryout point to a higher value heat input. A graph of $\dot{m}_{lt}$ vs. Q_{in} for various wick combinations would be a definitive display of pipe performance under these various conditions. The measurement of $\dot{m}_{lt}$ to the accuracy required here is impractical. However, an indication of the relative values of $\dot{m}_{lt}$ can be obtained from the data taken. Equation (22) represents the heat transferred from the evaporator to the vapor. Equation (12) represents the heat transferred by the vapor to the condenser. At steady state operating conditions, these two values are equal. Thus,

$$Q_e = \frac{2\pi L_t (T_e - T_v) k_w}{\ln (r_{wo}/r_{wi})} = H \dot{m}_{lt} \qquad (23)$$

Since π, L_t, H, k_w, and r_{wi} are constants,

$$\dot{m}_{lt} \propto (T_e - T_v) \qquad (24)$$

when r_{wo} is constant.

Here, r_{wo} represents the location of the liquid-vapor interface. It is not constant for all heat fluxes since the water level in the evaporator recedes with increasing heat flux [3]. Therefore, $\dot{m}_{lt}$ is not a linear

function of $(T_e - T_v)$. Since r_{wo} decreases with increasing Q_e, the graph of $(T_e - T_v)$ vs. Q_e will have an increasing slope as Q_e increases from zero. Additionally, an improving parameter change is expected to increase the maximum $\dot{m}_{lt}$, so a typical set of data will have three coinciding curves where an improving parameter change is indicated by an extension to a higher dryout point. Figure 12 shows a set of predicted data curves.

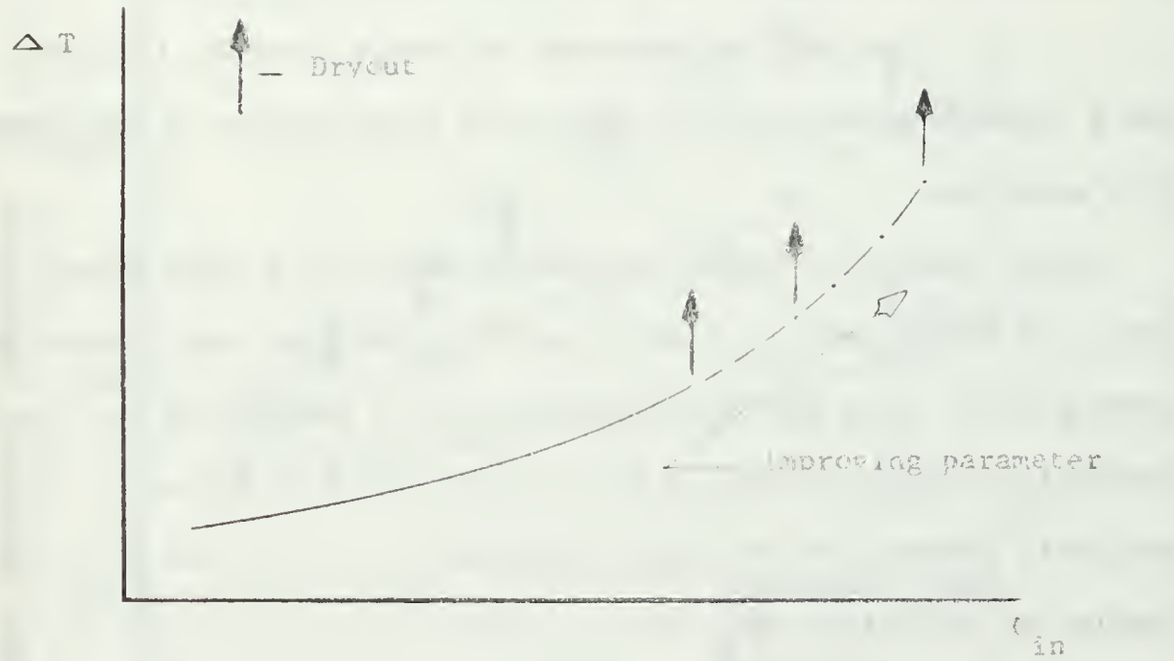

Figure 12 Predicted Data Curves

NOTE: An improved maximum $\dot{m}_{lt}$ is indicated by an extension of the basic curve and a larger Q at dryout.

B. NON-REPETITIVE DATA

As mentioned in the Experimental Procedure, the first set of data was non-repetitive. Figure 13 shows this data. This behavior was obtained by hot-start operation, that is, by not allowing the pipe to cool after filling and between runs. On each run the pipe was taken beyond dryout and the heat input was then adjusted back to the start point of 20 watts, with the air envelope adjusted accordingly. As shown

in Figure 13, the pipe settled at a higher T_e for each input wattage on each succeeding run. It appeared that by the fifth run, the upper limit of the hot-start operating line had been practically reached.

In searching for an explanation of the above-mentioned behavior, two possibilities were considered:

1. Non-condensables in the fluid had been trapped in the wick, inhibiting the flow of cooling fluid to the evaporator and building an insulating layer of air at the evaporator-wick interface.

2. The high temperatures of dryout produced localized boiling and a consequent formation of insulating vapor bubbles at the evaporator-wick interface.

Since possiblity number one should result in a reduced mass flow rate, the dryout point in that situation would have been reduced on succeeding runs. This was not the case, so this possibility was discarded. Possibility number two should have little effect on the mass flow rate, but could account for the higher temperature. To rid the wick of vapor bubbles, a cold-start operation was used; that is, the pipe was allowed to cool between runs to at least 100°F while the vapor temperature was maintained about 10°F above the pipe temperature to ensure bubble condensation. This procedure was subsequently followed before each run with the result that data became easily repetitive

C. EFFECT OF EVAPORATOR CAPILLARY PUMPING RADIUS, r_{cppe}

The effect of r_{cppe} is shown by Figure 14. This data was obtained by changing the evaporator top layer mesh size while keeping all other parameters constant. Generally, this data looks like the predicted data curves of Figure 12. The 150 mesh does not differ substantially from the 80 mesh curve, and this is expected since the space openings of these two meshes differ by only 25.5%.

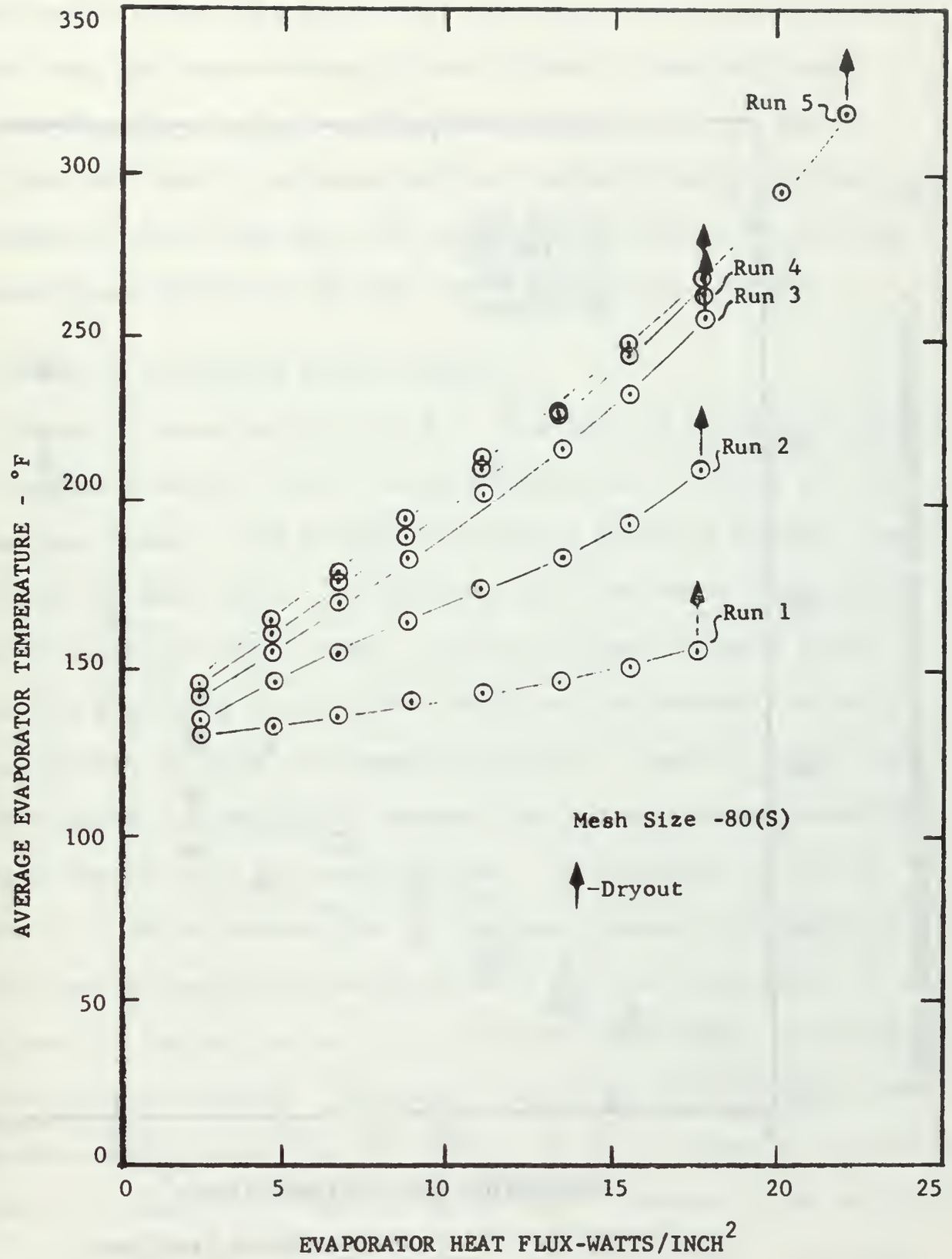

Figure 13. Effect of Hot-Start Operation

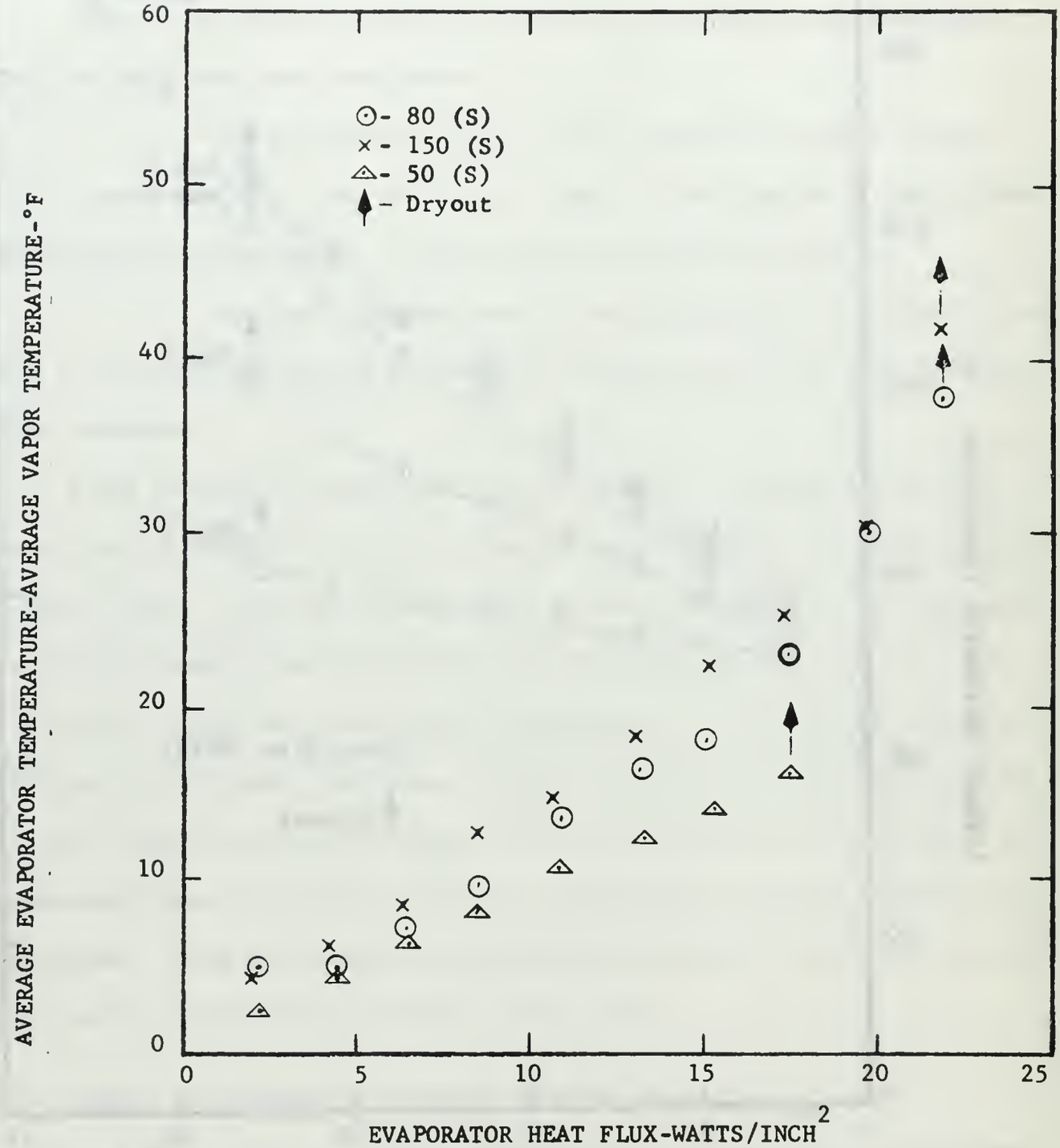

Figure 14. Effect of Evaporator Capillary Pumping Radius

The 50 mesh curve lies somewhat lower than the 80 mesh, and the dryout point is less than the 80 mesh. The lower dryout should be expected since the space opening for size 50 mesh is some 144% larger than the 80 mesh.

This data tends to substantiate the hypothesis that decreasing r_{cppe} increases the fluid flow rate. No explanation is offered for the lack of coincidence between the 50 mesh curve and the other two.

D. EFFECT OF EVAPORATOR WETTING ANGLE, θ_e

Figure 15 shows the effect of θ_e. This data was obtained by changing the evaporator top layer cleaning procedure while keeping all other parameters constant. The trends shown by this data vary somewhat from the predicted data curves. As expected, all three curves practically coincide except for dryout point. The Most Improved cleaning method definitely produced a higher dryout point than the Standard, which is to be expected if it can be assumed that the Most Improved method produced a smaller wetting angle. However, the Improved method curve indicates a reduced fluid flow rate at dryout. This behavior is not expected if it can be assumed that the Improved cleaning does produce a smaller wetting angle than the Standard. A pertinent observation at this point is that at the last five data points on this run, the evaporator was boiling violently. Fluid was being thrown out of the wick, and evaporator temperatures were oscillating 5 to 6°F. Because of the oscillations, the value of the data is questionable. Because of the boiling, the value of the data as an indication of fluid flow rate is certainly questionable. Figure 15 does not show conclusively the effect of the evaporator wetting angle. It does show, however, that the cleaning procedure significantly affects heat pipe performance.

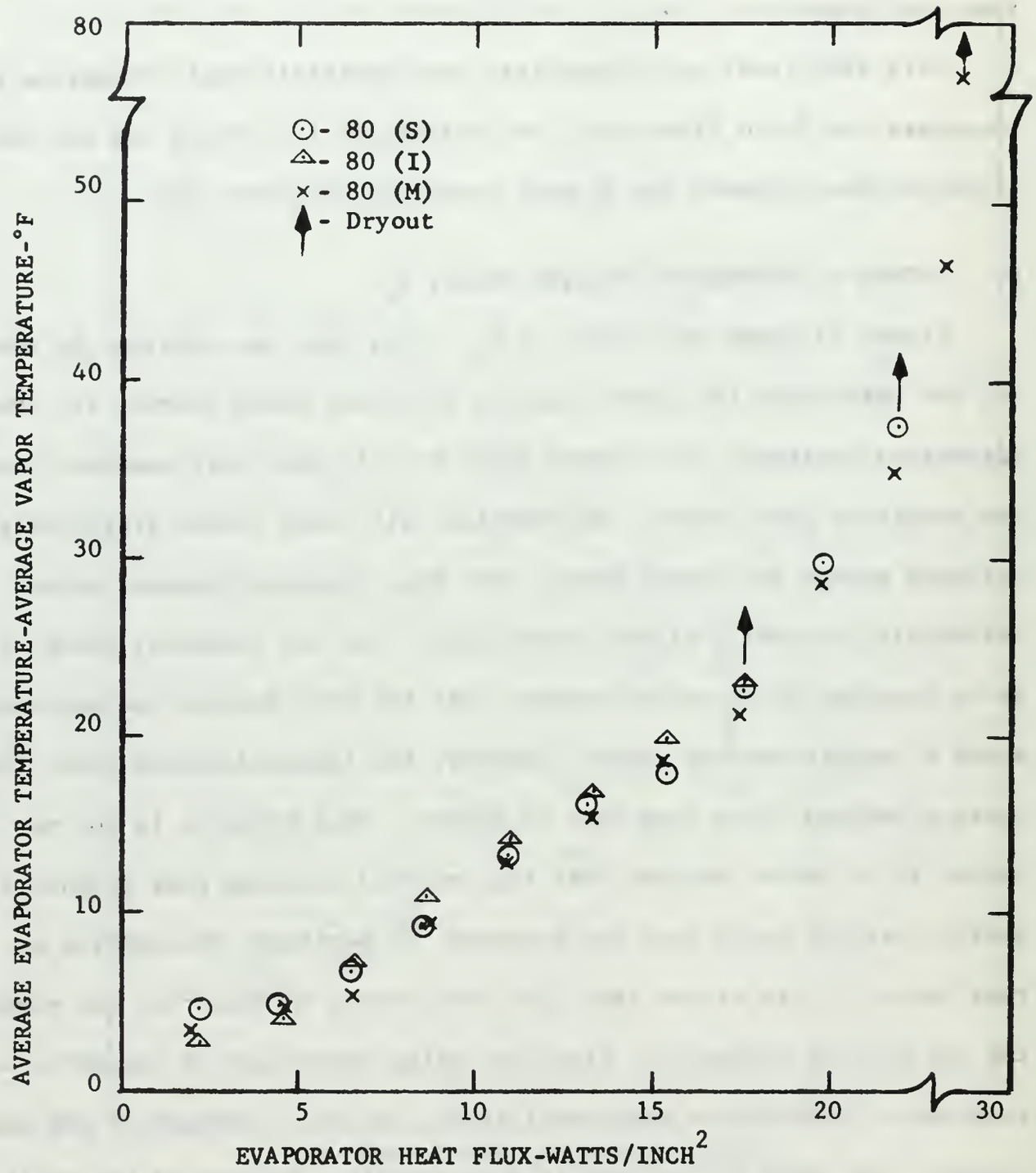

Figure 15. Effect of Evaporator Wetting Angle

E. EFFECT OF CONDENSER CAPILLARY PUMPING RADIUS, r_{cppcd}

The effect of r_{cppcd} is shown in Figure 16. This set of data varies considerably from the predicted curves. The 50 mesh dryout is lower than expected. On these 50 mesh runs, it was noted that the 50 mesh top layer did not fill completely. Repeated attempts at refilling had no effect. In the absence of proper wick filling, the 50 mesh data must be discounted.

With typical hindsight, the r_{cppmax} was computed for a wick thickness of .1 inch. Approximating r_{cpp} by one-half the mesh spacing, and using Equation (20) for r_{cppmax}, a comparison showed that none of the wire meshes should hold a .1 inch thick wick completely full. Yet, except for the case of the 50 mesh in the condenser, all wick combinations did hold the water. This contention was verified by visual observation through a magnifying glass. It appears that equation (20) is too conservative, and that there is some additional holding mechanism not considered by the development of this equation.

The 150 mesh data curve also does not fall as expected. From the predicted data, the 150 mesh curve should coincide with the 80 mesh curve. The dryout point did fall short of the 80 mesh, as was expected. However, as was the case with the 80 (I) mesh in the evaporator, this set of data was taken with violent boiling and temperature oscillations in the evaporator. Consequently, this data must also be discounted. No conclusions may be drawn from Figure 16 regarding the effect of the condenser capillary pumping radius.

F. EFFECT OF WICK AGING

As mentioned earlier, some runs were accompanied by violent boiling and evaporator temperature oscillations. This occurred on wick

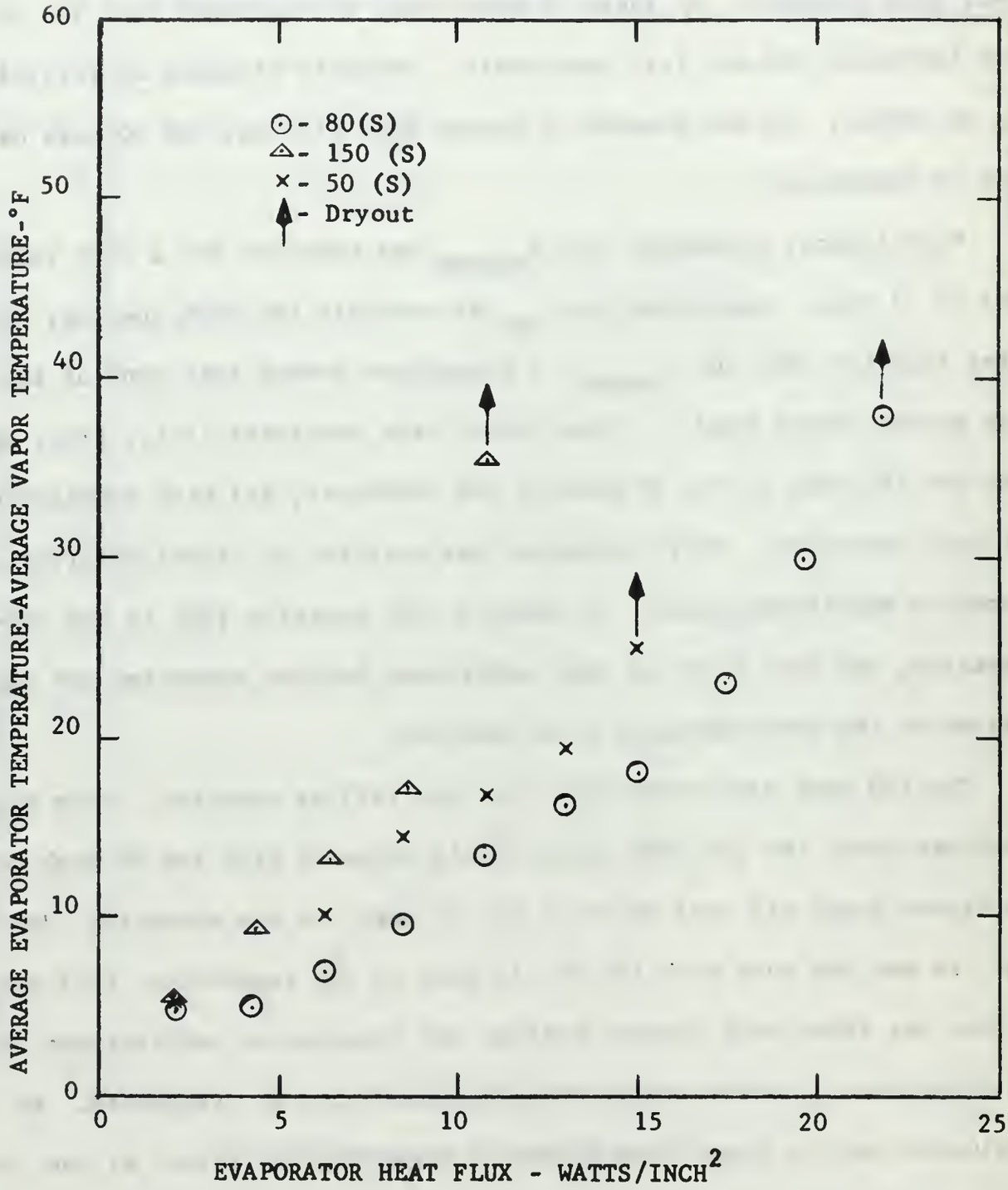

Figure 16. Effect of Condenser Capillary Pumping Radius

combination numbers 4, 6, and 7, as listed in Table 2. This behavior reached its most violent proportions, and the data deviated most from the predicted curves, on run number 7. Since the boiling precluded the gathering of data useful to the intended investigation, the remainder of the investigation was devoted to the boiling.

At first, it was thought that the boiling might be due to an accumulation of non-condensables in the evaporator. The non-condensables could have acted simultaneously to raise the $T_e - T_v$ by insulating the water from the pipe, and to serve as nucleation sites. To remove any non-condensables, the wick was dried out completely overnight by use of the evaporator heater and a continuous vacuum on the vapor space. After refilling by the usual procedure, additional data was taken. No changes in behavior or data values were noted. This ruled out non-condensable build-up as a cause of the boiling. A possible contribution by vapor bubbles caused by hot-start operation had already been eliminated by the standard operating procedure of cooling the pipe between runs.

Next, the possibility was considered that wick aging might be a factor. It was noted that at this point some 55 runs had been made on the same basic wick. Numerous exposures to the atmosphere had taken place while repairs to the equipment or top layer changes were made. Such usage and exposure were very likely to alter the chemical characteristics of the wick surface. To investigate this possibility, the top layer of the wick was removed and the chemical treatment part of the Improved Cleaning method was repeated with the basic wick in place on the pipe. The top layer was then replaced, the pipe refilled and additional data taken. There was a notable reduction in the boiling activity and an increase in the dryout point.

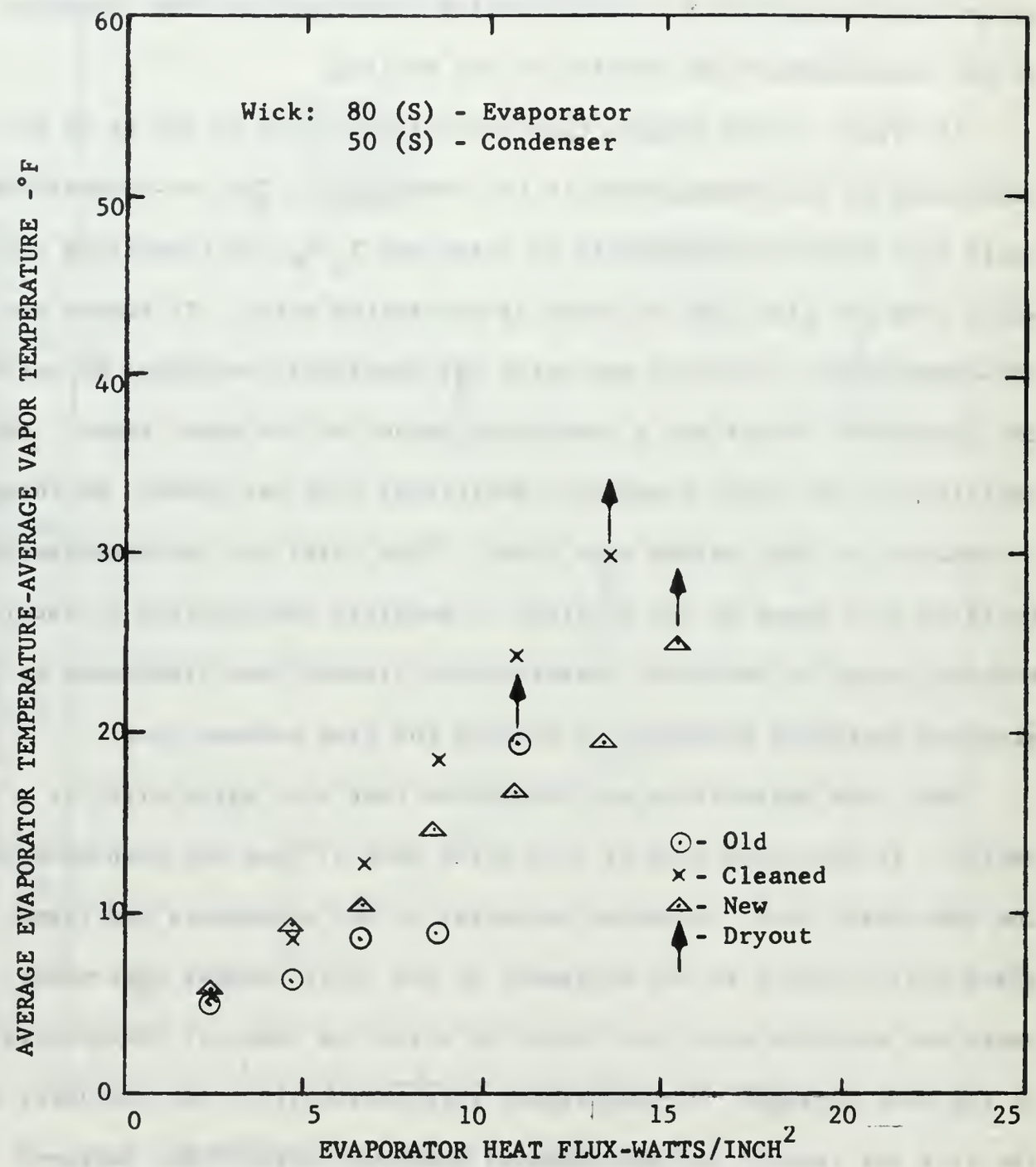

Figure 17. Effect of Wick Aging

These results stimulated the thought that a new wick might show the trend even more emphatically. Consequently, a new wick, identical to the old, was constructed, cleaned and installed. The pipe was refilled and additional data taken. Figure 17 shows the results of data taken for all three situations. The cleaned old wick shows an improved dryout point. The new wick shows an even more improved dryout and a more typical curve. Furthermore, the new wick showed no inclination to boil. This new wick data was used in Figure 16 to show the effect of r_{cppcd}.

The trend toward higher dryout points, plus the progressive elimination of boiling, shows that the wick experienced a detrimental aging effect. Whether the aging effect was due to atmospheric exposure, long-term usage, or a combination of the two cannot be determined by data taken in this investigation.

G. CORRELATION WITH PREVIOUS INVESTIGATION

The basic mesh size and wick thickness for this investigation were chosen specifically for the purpose of comparing data with a predecessor on this equipment, H. E. Kilmartin. Kilmartin's work included a constant pressure run at 25 inches Hg vacuum on an 80 mesh, .1 in. thick wick. The data taken by this investigator was on the same basic wick at constant volume. Pressures varied from about 27 inches Hg vacuum to about 24 inches Hg vacuum. Figure 18 shows a comparison with Kilmartin's data.

This investigator's data fell from about 12°F to 25°F below that of Kilmartin, while the dryout point was at about 22 watts/inch^2 versus 12 watts/inch^2 for Kilmartin. This represents improved performance since more heat is transferred at the same temperature as Kilmartin's, and since the dryout point was considerably extended beyond Kilmartin's.

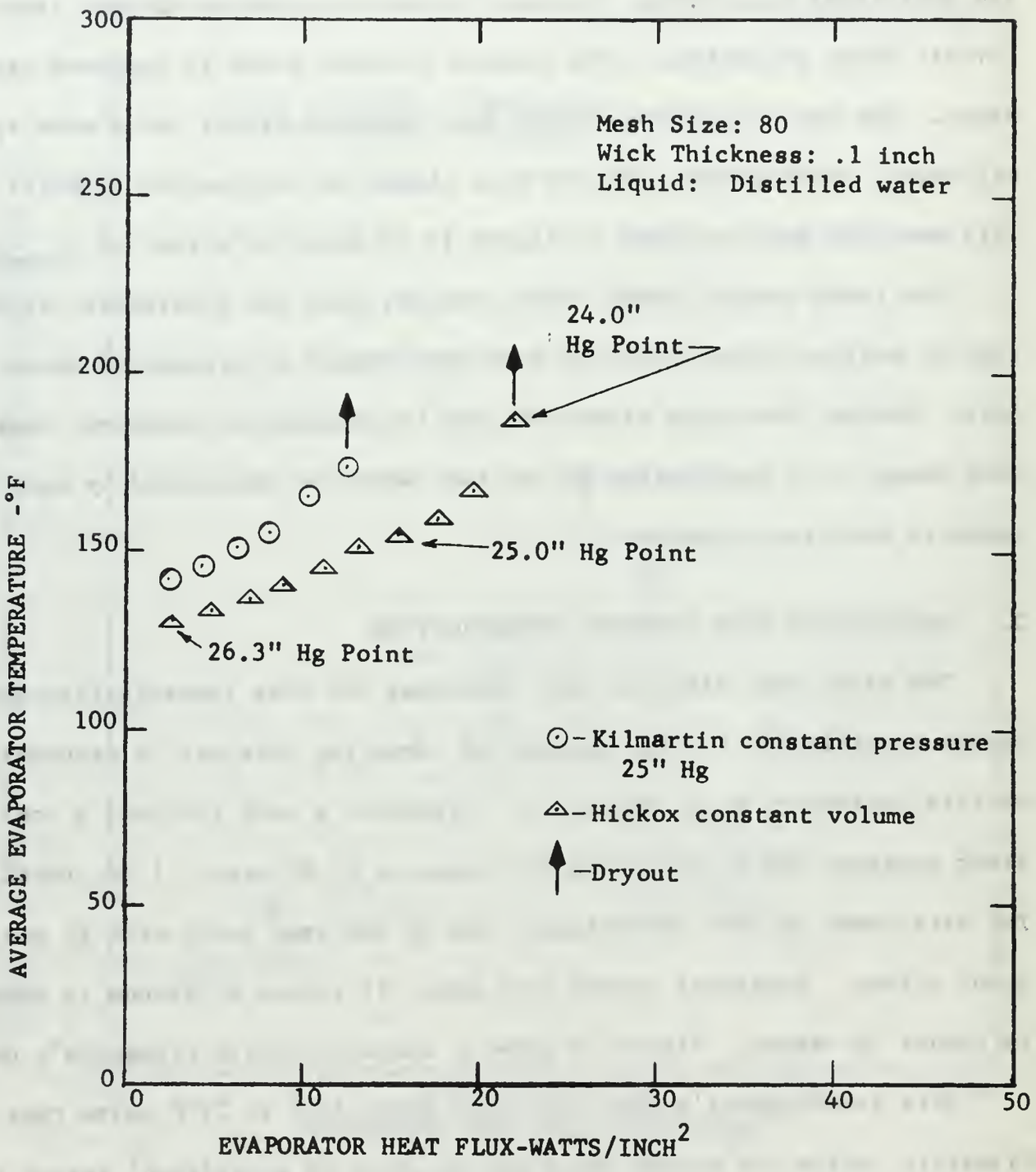

Figure 18. Data Correlation

There are two likely reasons for the improved performance. One is that the filling and purging procedure removes more non-condensables from the liquid than Kilmartin's procedure. This seems likely, since Kilmartin made no specific effort to remove non-condensables from the working fluid. By boiling the liquid for at least 15 minutes before filling the wick, as was done in this investigation, the majority of non-condensables entrained in the liquid were released. As suggested by Kunz et al [10], non-condensables may build up in the wick, restricting the fluid flow. This type of behavior seems evident in Kilmartin's case since his curve has a higher slope and lower dryout point. The effect is even more marked when it is pointed out that, all other things being equal, this investigator's curve should have had a higher slope than Kilmartin's. It should have started below his curve, crossed at the common pressure point, and continued above to dryout. Kilmartin's data shows more tendency toward fluid flow restriction with increasing heat flux than does data obtained here.

The other likelihood is that the wick assembled by this investigator was not as tightly wound as Kilmartin's, creating larger axial passages, thereby reducing the fluid flow resistance. This possibility, though feasible, does not seem as likely as the first, since the wick was wound tightly and spot-welded in place.

The more logical explanation for improved performance is that it is due to the more effective purging and filling procedure used in this investigation.

H. GENERAL OBSERVATIONS

Several of the interesting phenomena observed did not fit easily into a specific area of discussion, yet they are of such interest that they

should be discussed. Accordingly, this section includes a discussion of several observed phenomena which are not necessarily closely interrelated.

1. Water Level

Visual observation showed that, except for the one case in which the wick did not fill properly, the water level never receded below the top layer in the wick. It could be seen that, as the heat input increased toward dryout, the water level receded slightly, but never did it recede below the top layer.

2. Boiling

On about the latter two-thirds of most runs, even though violent boiling was not in evidence, there was a tendency at the beginning of each new heat input step for the water to surge slightly or to splash a very small amount into the vapor space. Usually, this happened only once or twice at each step, immediately after the heat input increase, with no further agitation. No temperature oscillations were noted during these episodes.

This behavior suggests that either film or nucleate boiling may be taking place at the pipe-liquid interface over a relatively wide range of heat fluxes. Either case would have the same effect if the bubbles from nucleate boiling are of sufficient size to be trapped at the wick-pipe interface. This possibility is reinforced by the fact that the water level does not recede appreciably, even at dryout. Recalling that the drop in water level was expected to account for the change in slope of the predicted data curves shown in Figure 12, it appears that the minute water level drop observed visually could not account for a large departure from linearity. A water level drop into the second mesh layer would cause about a 14% increase in the slope. The actual change in slope of the size

80 (S) curve in Figure 14 is about 280%. There is apparently another cause of non-linearity. A vapor pocket could be responsible.

3. Fluid Displacement from the Wick

On most runs, at the third or fourth data step, water was slowly pushed from the wick at the condenser end. The amount of water displaced was seen to be a non-linear function of the heat input, with larger amounts observed at first, then succeedingly smaller amounts appearing as the heat input was increased. When violent boiling began, the amount of water present outside the wick did not change with heat input.

This is more evidence in behalf of the boiling hypothesis. Perhaps, as boiling begins, a vapor film, or pocket, is formed at the pipe-liquid interface in the evaporator. As heat input is increased, the vapor pocket grows, displacing fluid. If the wick is initially full, the displaced fluid must leave the wick. Due to equipment construction, the pipe was operated throughout with a very slight tilt down at the condenser end. Hence, the fluid emission at that end. The non-linearity of the amount displaced might be explained by a compression effect. As the vapor pocket grows, the capillary holding power of the wick compresses the pocket, so that each succeeding heat input expands the pocket by a smaller amount, pushing out less fluid than the previous input. When violent boiling takes place, the vapor escapes through the wick and no additional fluid is pushed from the wick.

4. Movement of Boiling Center

On one occasion of violent boiling, it was noted that the apparent center of boiling action progressed from its location at the center of the evaporator to a position more toward the evaporator-condenser interface. No explanation is offered for this behavior.

5. Fin Effect of Wick

There is another possible contribution to radial heat transfer that has not been considered, the fin effect of the wick. It has been thought that the poor physical continuity between pipe, wick and adjacent layers of the wick would negate any sizeable contribution of a fin effect. It is possible, however, that with a relatively high thermal conductivity for the wick material and a low conductivity for the fluid, the fin effect may be significant. This fact is particularly pertinent in this case where k for water $\simeq$ .37Btu/hr-ft-°F and k for nickel $\simeq$ 40 Btu/hr-ft-°F. Theoretical predictions for this effect are not practical due to the geometrical configuration of the wick.

It is worth noting that the adverse wick aging effect observed may indicate a significant fin effect. It was found that the age or condition of wick surface was directly related to the amount of violent boiling in the evaporator. If the wick does have a sizeable fin effect, then the formation and growth of an oxide or other chemical combination on the wick surface would reduce the contribution of the fin effect. This is in agreement with the vapor pocket hypothesis, since a reduction in fin effect would necessitate a greater heat transfer contribution by the pipe-liquid interaction. Hence, higher temperature differences at the pipe-liquid interface, and more violent boiling.

Although there is no conclusive evidence in support of the wick fin effect hypothesis, there is sufficient evidence of the possibility that it does apply to warrant further investigation into that possibility.

6. Condenser Inactive Region

There was no noticeably well-defined demarcation line separating the active and inactive regions of the over-designed condenser

such as that noticed by Mosteller [3]. The concentration of condensation in the condenser seemed to decrease linearly with distance from the condenser-evaporator interface, approaching zero some four to five inches from the condenser end.

VI. CONCLUSIONS AND RECOMMENDATIONS

A. CONCLUSIONS

From the data and behavior observed in this heat pipe, the following conclusions are offered:

1. Decreasing the evaporator capillary pumping radius improves pipe performance.

2. Removal of non-condensables from the working fluid significantly improves pipe performance.

3. The mechanism which holds the working fluid in the wick includes some other phenomena in addition to the surface tension effect.

4. The wick cleaning method has a significant effect on heat pipe operation.

5. There is evidence that a vapor film, or pocket, forms in the evaporator at the pipe-liquid interface over a wide range of heat fluxes.

6. Continued use, exposure to the atmosphere, or a combination of both leads to a detrimental aging of a nickel wire mesh wick cleaned by the Improved method. This aging produces a progressive violent boiling in the evaporator.

7. There is evidence that the fin effect of the wick may be a substantial contribution to radial heat transfer when the thermal conductivity of the wick material is relatively high compared to that of the working fluid.

B. RECOMMENDATIONS FOR FURTHER STUDY

1. Continue investigation of the effect of the evaporator and condenser wetting angles, the condenser capillary pumping radius, and the capillary frictional radius. The wick aging problem may be avoided by renewing the entire wick on each wick combination change.

2. In conjunction with number one, investigate more fully the mechanism that holds the working fluid in the wick. Revise the limits of the capillary radii accordingly.

3. Investigate the possibility of film boiling at the evaporator-liquid interface. This could be done with a glass construction, standard heat pipe utilizing a radiation heat source which would allow adequate maneuvering room for a small periscope or mirror to be used for visual perusal of the evaporator-liquid interface at operating conditions.

4. In conjunction with number three, investigate the effect of hot-start operation on the pipe by using various combinations of heat input increase and decrease steps. Determine if a vapor pocket forms only at or above dryout. Determine if there is a limiting hot-start operation curve and if the pipe will operate on that curve with continuous operation, or if it shows a "hysteresis" effect.

5. Investigate the fin effect of the wick. This can be done by using various methods for thermally bonding to or insulating the wick from the pipe.

APPENDIX A

COMPUTING THE RELATIVE MAGNITUDE OF $\frac{\Delta P_v}{\Delta P_l}$

Dividing equation (4) by equation (7),

$$\frac{\Delta P_v}{\Delta P_l} = \frac{8}{K_1} \frac{\rho_l}{\rho_v} \frac{\mu_v}{\mu_l} \frac{(r_{wo}^2 - r_{wi}^2)}{(r_g^2 + r_{wo}^2 - 2r_{vlm}^2)(r_g^2 - r_{wo}^2)}$$

$$\text{where } r_{vlm}^2 = \frac{r_g^2 - r_{wo}^2}{\ln(r_g/r_{wo})^2}$$

For Water at 300°F [12]	For Saturated Steam at 300°F [12]
$\rho_l = 57.3$ lbm/ft^3	$\rho_v = .155$ lbm/ft^3
$\mu_l = .45$ lbm/ft-hr	$\mu_v = .0337$ lbm/ft-hr

For the dimensions of the Apparatus	For the Wick [10]
$r_{wi} = .375$ inches	$K_{lmin} = 1.4 \times 10^8/\text{ft}^2$
$r_{wo} = .475$ inches	
$r_g = .655$ inches	

$$\frac{\Delta P_v}{\Delta P_l} \simeq \frac{(8)(144)(57.3)(.0337)(.475^2 - .375^2)}{(1.4\times10^8)(.155)(.45)(.655^2 + .475^2 - 2\,\frac{.428 - .226}{\ln(\frac{.655}{.475})^2})(.45 - .226)}$$

$$\frac{\Delta P_v}{\Delta P_l} \simeq 2.39\times10^{-4}$$

Note that ΔP_v and ΔP_l will be the same order of magnitude if $K_l \simeq 10^4$.

APPENDIX B

MENISCUS - RADIUS RELATIONSHIPS

Consider a meniscus between the parallel wires of a wire mesh wick with zero wetting angle.

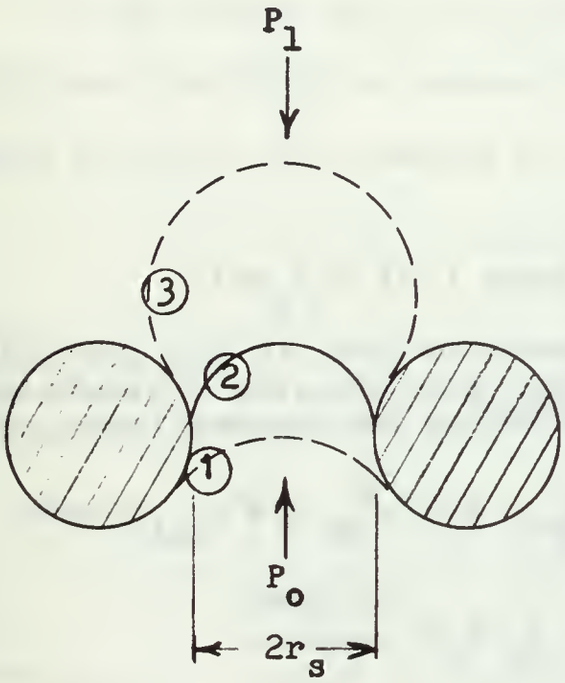

Case 1. $P_l < P_o$

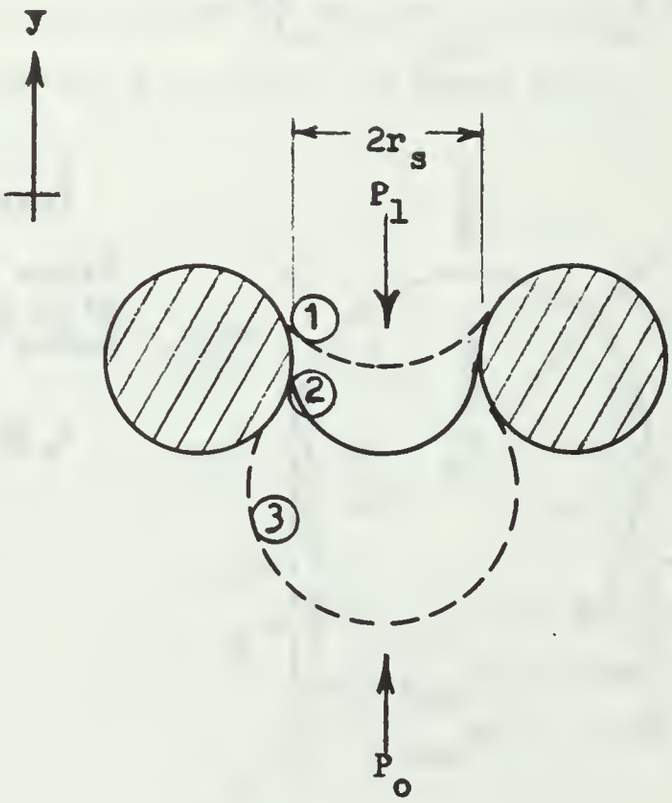

Case 2. $P_l > P_o$

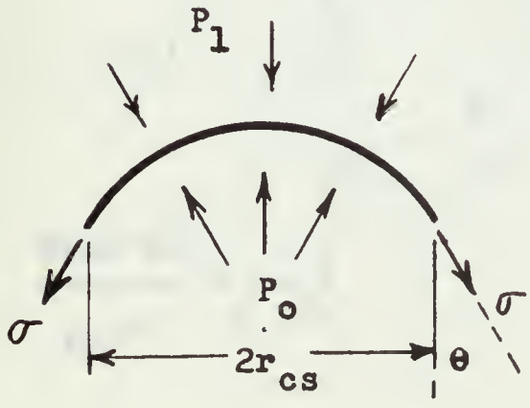

At equilibrium, $\Sigma F_y = 0$

Take Case 1-1:

$$P_o \pi r_{cs}^2 - P_l \pi r_{cs}^2 - 2\sigma \pi r_{cs} \cos\theta = 0$$

$$P_o - P_l = \frac{2\sigma \cos\theta}{r_{cs}}$$

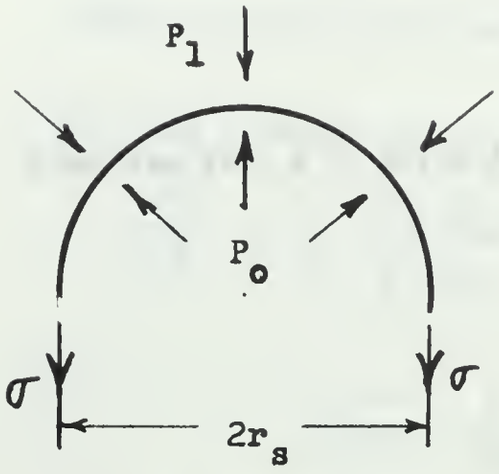

Take Case 1-2: $\Sigma F_y=0$:

$$P_o\pi r_s^2-P_1\pi r_s^2-2\sigma\pi r_s=0$$

$$P_o-P_1=\frac{2\sigma\,Cos\theta}{r_s}$$

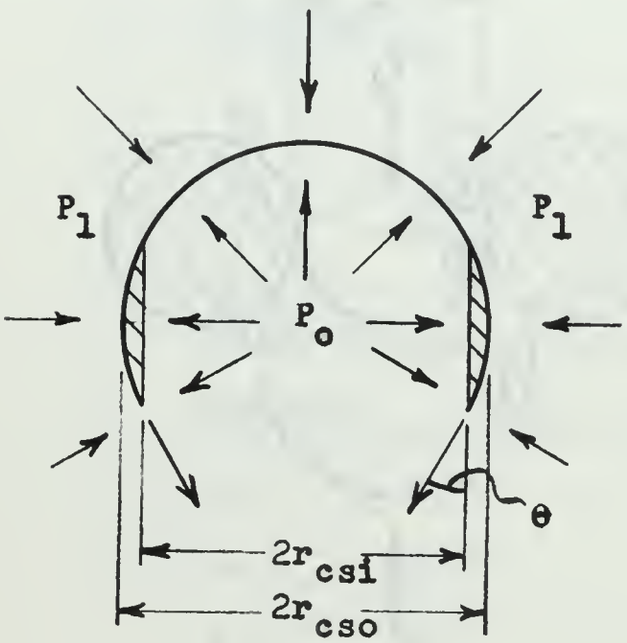

Take Case 1-3: $\Sigma F_y=0$:

Since pressure acts in all directions with equal strength, the cross-hatched areas offer no net upward force. So,

$$P_o\pi r_{csi}^2-P_1\pi r_{csi}^2-2\sigma r_{csi}Cos\theta=0$$

$$P_o-P_1=\frac{2\sigma\,Cos\theta}{r_{csi}}$$

Case 2 will lead to the same result with a negative sign on the right. Compare cases 1-1, 1-2, and 1-3.

1-1	1-2	1-3
$P_o-P_1=\frac{2\sigma\,Cos\theta}{r_{cs}}$	$P_o-P_1=\frac{2\sigma}{r_s}$	$P_o-P_1=\frac{2\sigma\,Cos\theta}{r_{csi}}$

It can be seen that both r_{cs} and $r_{csi} > r_s$ and that $\cos\theta < 1$. Therefore, case 1-2 represents the most stable case and $r_{min} = r_{spacing}$. Additionally, note that case 1-3 cannot represent an equilibrium situation since the higher $\triangle P$ required to produce that meniscus shape will be sufficient to collapse the meniscus.

If the wetting angle is not zero, but θ', the above relationships hold where the effective wetting angle is the sum of the actual wetting angle θ' and the local surface inclination ϕ, or, from the sketch below,

$$\theta = \theta' + \phi$$

and,

$$r_{cs} = r_{wr}(1-\cos\phi) + r_s = r_m\cos\theta$$

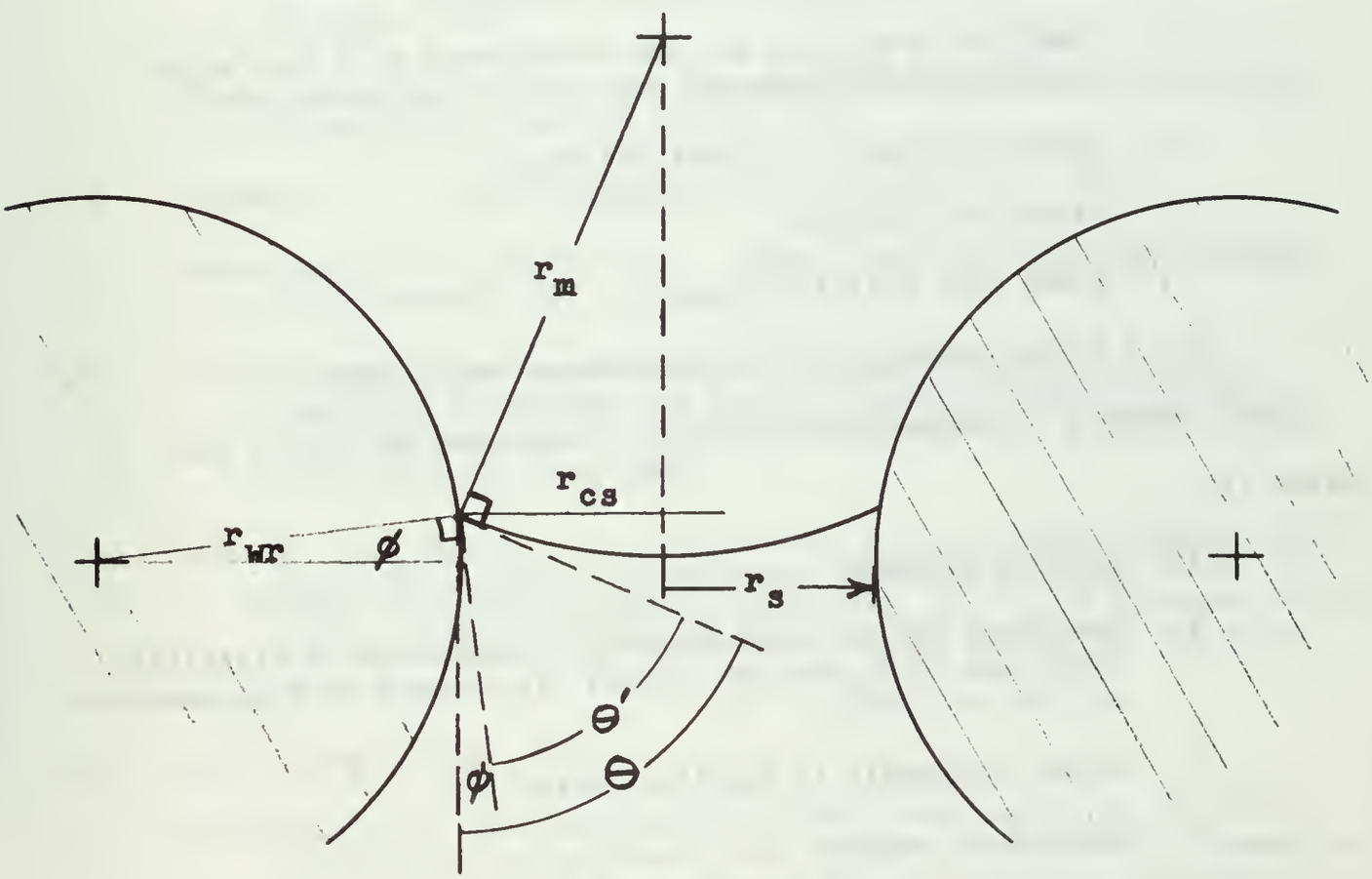

APPENDIX C

CLEANING PROCEDURES

STANDARD

1. Scrub in hot water and Alconox, a commercial wetting agent.
2. Clean ultrasonically for 30 minutes.
3. Rinse thoroughly with distilled water.
4. Rinse with acetone.
5. Rinse with distilled water.
6. Store submerged in distilled water until used.

IMPROVED - Recommended by the Jet Propulsion Laboratory for Stainless Steel [13].

1-3. Same as STANDARD.

4. Soak for 20 minutes at room temperature in a bath of 30 cc Sodium Dichromate and one liter of Sulphuric Acid.
5. Rinse thoroughly in distilled water.
6. Rinse with acetone.
7. Rinse with distilled water.
8. Store submerged in distilled water until used.

MOST IMPROVED - Recommended by the Jet Propulsion Laboratory for Nickel [13].

1-3. Same as STANDARD

4. Passivate for 30 to 60 minutes in a solution of distilled water and 20 to 40% (by volume) nitric acid at a temperature of 130° to 160°F.
5. Rinse thoroughly in distilled water.
6. Rinse with acetone.
7. Rinse with distilled water.
8. Store submerged in distilled water until used.

BIBLIOGRAPHY

1. Feldman, K. T., Jr., Heat Pipe Analysis, Design and Experiments, Scott Engineering Sciences, December 1968.

2. Grover, G. M., Cotter, T. P., and Erickson, G. F., "Structures of Very High Thermal Conductance," Journal of Applied Physics, Vol. 35, 1964.

3. Mosteller, W. L., The Effect of Nucleate Boiling on Heat Pipe Operation, M. S. Thesis, Naval Postgraduate School, Monterey, 1969.

4. Kilmartin, H. E., Jr., The Effect of Wick Geometry on the Operation of a Longitudinal Heat Pipe, M. S. Thesis, Naval Postgraduate School, Monterey, 1969.

5. Longwell, Paul A., Mechanics of Fluid Flow, McGraw-Hill, Inc., 1966.

6. Busse, C. A., "Pressure Drop in the Vapor Phase of Long Heat Pipes," Thermionic Conversion Specialist Conference Record of IEEE, 1967.

7. Scheidegger, Adrian E., The Physics of Flow Through Porous Media, University of Toronto Press, 1960.

8. Chapman, A. J., Heat Transfer, The MacMillan Co., 1967.

9. Rohsenow, W. M., and Choi, H., Heat, Mass, and Momentum Transfer, Prentice-Hall, Inc., 1961.

10. Lewis Research Center, NASA CR-812, Vapor-Chamber Fin Studies, Transport Properties and Boiling Characteristics of Wicks, by H. R. Kunz, L. S. Langston, B. H. Hilton, S. W. Wyde, and G. H. Nashick, June 1967.

11. Ginwala, K., Blatt, T. A., and Bilger, R. W., Engineering Study of Vapor-Cycle Cooling Components for Space Vehicles, Tech. Doc. Repts. No. ASD-TDR-630582, Sept 1963, AF Flight Dynamics Laboratory, Air Force Systems Command, Wright-Patterson Air Force Base, Ohio.

12. ASME Steam Tables, 1967.

13. Jet Propulsion Laboratory Letter JS:sp, with enclosure JPL Proc. KP504273 A, to Professor Paul J. Marto, Mechanical Engineering Department, Naval Postgraduate School, Subject: Heat Pipe Cleaning Procedures, 8 July 1969.

INITIAL DISTRIBUTION LIST

		No. Copies
1.	Defense Documentation Center Cameron Station Alexandria, Virginia 22314	20
2.	Library, Code 0212 Naval Postgraduate School Monterey, California 93940	2
3.	Naval Ship Systems Command, Code 2052 Code 31, Department of the Navy Washington, D. C. 20360	1
4.	Mechanical Engineering Department Naval Postgraduate School Monterey, California 93940	2
5.	Professor P. F. Pucci Mechanical Engineering Department Naval Postgraduate School Monterey, California 93940	2
6.	Professor P. J. Marto Mechanical Engineering Department Naval Postgraduate School Monterey, California 93940	1
7.	LT O. J. Hickox, Jr., USN Boston Naval Shipyard Boston, Massachusetts 02110	2

DOCUMENT CONTROL DATA - R & D

(Security classification of title, body of abstract and indexing annotation must be entered when the overall report is classified)

1. ORIGINATING ACTIVITY *(Corporate author)*
Naval Postgraduate School
Monterey, California 93940

2a. REPORT SECURITY CLASSIFICATION
Unclassified

2b. GROUP

3. REPORT TITLE
A Study of Wire Mesh Wick Characteristics in a Longitudinal Heat Pipe

4. DESCRIPTIVE NOTES *(Type of report and, inclusive dates)*
Master's Thesis; December 1969

5. AUTHOR(S) *(First name, middle initial, last name)*
Oscar Jonathan Hickox, Jr., USN

6. REPORT DATE	7a. TOTAL NO. OF PAGES	7b. NO. OF REFS
December 1969	71	13

8a. CONTRACT OR GRANT NO.

b. PROJECT NO.

c.

d.

9a. ORIGINATOR'S REPORT NUMBER(S)

9b. OTHER REPORT NO(S) *(Any other numbers that may be assigned this report)*

10. DISTRIBUTION STATEMENT
This document has been approved for public release and sale, its distribution is unlimited.

11. SUPPLEMENTARY NOTES

12. SPONSORING MILITARY ACTIVITY
Naval Postgraduate School
Monterey, California 93940

13. ABSTRACT

An everted, glass-enclosed, nickel heat pipe was operated at constant volume using a nickel wire mesh wick and distilled water. The performance of the pipe was evaluated under various combinations of wick parameters. The effect of the radial evaporator capillary radius, the radial condenser capillary radius, and the evaporator wetting angle were investigated at a pressure range of 27 to 24 inches of Mercury vacuum.

The performance of the pipe was found to improve with decreasing radial evaporator capillary radius and decreasing amounts of non-condensables in the working fluid. A detrimental wick-aging effect which led to violent boiling and early dryout was observed.

A discussion of observed behavior presents evidence that boiling and wick fin effect may play a significant part in heat pipe operation.

14 KEY WORDS	LINK A		LINK B		LINK C	
	ROLE	WT	ROLE	WT	ROLE	WT
Heat Pipe						
Wire Mesh Wick						
Radial Capillary Pumping Radius						
Axial Capillary Frictional Radius						
Wetting Angle						
Heat Transfer						

Thesis
H5268
c.1

118953

Hickox
A study of wire mesh wick characteristics in a longitudinal heat pipe.

Thesis
H5268
c.1

Hickox
A study of wire mesh wick characteristics in a longitudinal heat pipe.

118953